



Master's Thesis in Electrical Engineering, 30 ECTS

---

**Stochastic Knock Control for Improved  
Efficiency**

---

Jonas Vedin, Robert Widén

**LiTH-ISY-EX-19/5228-SE**

June, 2019

Master's thesis, Civilingenjörsprogrammet i Maskinteknik, Linköpings University.  
Jonas Vedin, jonve231@student.liu.se, Robert Widén, robvi186@student.liu.se.

*Stochastic Knock Control for Improved Efficiency* is a project done in the course Examensarbete (TQET33) in Mechanical Engineering, 30.0 ECTS at the *Department of ISY*, Linköping University.

Supervisors: Fredrik Wemmert (*Engine control*, Volvo Car Corporation) and Robin Holmbom (*Department of Physics*, Linköping University)  
Examiner: Lars Eriksson (*Department of ISY*, Linköping University.)

*“So much good, so much evil. Just add water.”*

–Markus Zusak, *The Book Thief*

---

## Abstract

Increasing the efficiency and performance of internal combustion engines is always of interest in the automotive industry. One limiting factor to achieve this in gasoline combustion engines is the ignition timing which can not always be set where optimal ignition efficiency and performance is obtained. This is due to the knock phenomenon which is an abnormal combustion process that can damage the engine. Due to knock, a feedback controller which sets the ignition timing at the best possible value without the risk of harming the engine is required. In this thesis, a statistically driven knock intensity simulation environment based on the Burr Type XII distribution model was set up. In the simulation environment, different stochastic knock feedback controllers were implemented along with background noise estimation techniques used in the knock detection system. The feedback controllers were evaluated against the conventional knock controller commonly used in today's engines in terms of ignition angle and transient response. The results from the simulation environment showed that a more advanced mean ignition angle can be achieved with stochastic based knock control strategies with the same knock-rate and without lessening the fast transient response achieved from the conventional strategy. To evaluate the results, some of the controllers were implemented in a four cylinder two-liter four stroke Volvo engine with similar results.

*“Only those who will risk going too far can possibly find out how far one can go.”*

–T.S. Eliot

# Acknowledgement

---

First and foremost, we would like to thank our supervisors Fredrik Wemmert and Robin Holmbom for all the support and guidance we have received throughout our progression with this master thesis. We would also like to thank Anders Bärås for taking your time to support us during the implementation phase of the new softwares. Also, we would like to thank our examiner Lars Eriksson at LiU and our group manager Frederik Falk at Volvo Cars for giving us this opportunity.

We would also like to thank our friends and family for the continuous love and support.

Jonas Vedin, Robert Widén  
Göteborg, Sweden,  
12 June, 2019.

# Contents

<b>1</b>	<b>Introduction</b>	<b>2</b>
1.1	Background . . . . .	2
1.2	Problem formulation . . . . .	2
1.3	Purpose and goals . . . . .	2
1.4	Approach . . . . .	3
<b>2</b>	<b>Related Research</b>	<b>4</b>
2.1	Knock . . . . .	4
2.2	Knock Signal Treatment and Detectability . . . . .	5
2.3	Knock Control . . . . .	6
2.3.1	Commonly used control algorithm . . . . .	7
2.3.2	Statistically Based Control Algorithms . . . . .	8
2.3.3	Threshold Optimisation . . . . .	8
2.3.4	Stochastic Knock Control . . . . .	8
2.4	Knock Intensity Distribution . . . . .	9
2.5	Knock Simulation . . . . .	9
<b>3</b>	<b>Theory</b>	<b>10</b>
3.1	Knock Detection . . . . .	10
3.1.1	Low-pass filter . . . . .	10
3.1.2	Fixed-step Background Noise Estimation . . . . .	11
3.2	Stochastic Process Analysis . . . . .	11
3.3	Probability Distribution Fitting . . . . .	12
3.3.1	Burr Type XII Distribution Model . . . . .	12
3.3.2	Log-normal Distribution Model . . . . .	13
3.3.3	Knock Intensity Error at the 95th Percentile . . . . .	14
3.3.4	Probability Error at Knock Event . . . . .	14
3.3.5	Kolmogrov-Smirnov Test Statistic . . . . .	14
3.4	Knock control . . . . .	15
3.4.1	Conventional Controller . . . . .	15
3.4.2	Cumulative Summation Based Control . . . . .	16
3.4.3	Likelihood Based Controller . . . . .	17
3.4.4	Threshold optimisation . . . . .	21
3.4.5	Cumulative summation based knock controller with likelihood-scaled controller gain and optimised threshold . . . . .	22
3.4.6	Live estimation of Burr Type XII distribution controller . . . . .	22
<b>4</b>	<b>Simulation Environment</b>	<b>23</b>
4.1	Overview of the simulation environment . . . . .	23
4.2	Simulation of Knock Intensity . . . . .	24
<b>5</b>	<b>Results</b>	<b>27</b>
5.1	Stochastic analysis . . . . .	27
5.2	Distribution Model Evaluation . . . . .	29
5.2.1	Knock Intensity Error at the 95th Percentile . . . . .	29

5.2.2	Probability Error at Knock Event . . . . .	31
5.2.3	Kolmogorov-Smirnov Test Statistic . . . . .	33
5.3	Knock Control . . . . .	34
5.3.1	Threshold Optimisation . . . . .	34
5.3.2	Conventional Knock Control . . . . .	35
5.3.3	Cumulative Summation Knock Control with Optimised Threshold and Likelihood-scaled Controller Gains . . . . .	37
5.3.4	Conventional Control with Optimal Threshold . . . . .	38
5.3.5	Likelihood knock control with fast-forward algorithm . . . . .	40
5.3.6	Live estimation knock control . . . . .	41
5.4	Side-by-side Comparison of Knock Controllers at Steady-state Operation . . . . .	43
5.5	Background noise evaluation . . . . .	46
<b>6</b>	<b>Discussion</b>	<b>48</b>
<b>7</b>	<b>Conclusions and Future Work</b>	<b>50</b>
7.1	Conclusions . . . . .	50
7.2	Future work . . . . .	51
	<b>Bibliography</b>	<b>52</b>
	<b>Appendix A Additional knock control results</b>	
A.1	Cumulative summation based knock control with likelihood-scaled control gains . . . . .	54
A.2	Cumulative summation based knock control with fast forward algorithm and likelihood-scaled controller gains . . . . .	55
A.3	Likelihood knock control . . . . .	56
A.4	Live estimation controller . . . . .	57
	<b>Appendix B Knock control results from real engine tests</b>	
B.1	Cummulative summation knock control with likelihood-scaled controller gains and optimised threshold . . . . .	58
B.2	Threshold optimised conventional controller . . . . .	59
B.3	Likelihood fast forward controller . . . . .	

# Nomenclature

---

## Abbreviations

<i>A/F</i>	Air-fuel
<i>CA</i>	Crank angle
<i>CDF</i>	Cumulative density function
<i>DBL</i>	Detection borderline
<i>EK</i>	Expected knock probability
<i>FIR</i>	Finite impulse response
<i>KP</i>	Knock probability
<i>KS</i>	Kolmogorov-Smirnov
<i>Ln</i>	Likelihood-ratio
<i>MBT</i>	Maximum brake torque
<i>PDF</i>	Probability density function
<i>SA</i>	Spark advance
<i>SAC</i>	Spark advance counter
<i>SI</i>	Spark-Ignition
<i>SKC</i>	Stochastic knock control
<i>SKD</i>	Stochastic knock detection
<i>TDC</i>	Top dead centre



# Chapter 1

## Introduction

---

### 1.1 Background

Fuel efficiency, engine performance and engine durability are always in need of improvement. Therefore a continuous development and investigation in improving the combustion process lies in interest for automotive developers. The limitation on combustion efficiency due to engine knock is well known and a closed loop control is indisputably required to maintain engine health and prevent engine failure. Such systems have been used in production vehicles for over 30 years. However, the control strategy and knock sensor treatment has remained relatively stagnant in improvement. Several publications have suggested new types of knock control algorithms that challenges the conventional strategies and indicates a potential for improved engine efficiency and performance.

### 1.2 Problem formulation

For internal combustion engines, optimising the spark timing is an important factor to maximise the engine power output, thermodynamic efficiency and fuel economy. However, the optimal spark advance is often not achievable due to the occurrence of knock. Therefore, a trade off is required in engine control where a spark advance that leads to Maximum Brake Torque (MBT) is weighted towards avoiding knock that can damage the engine. Knock occurs when a significant portion of the end-gas ahead of the flame front spontaneously ignites due to high in-cylinder temperature and pressure. By retarding the ignition angle it is possible to influence how the fuel is burnt in relation to the crank rotation, thus affecting the in-cylinder pressure and temperature. Knock control can be a challenging task due to the difficulty in handling the knock phenomenon and the stochastic characteristics of the combustion process. By implementing a knock event generator in Simulink, hopes are that an improved knock control strategy that increases engine efficiency can be developed.

### 1.3 Purpose and goals

The purpose of this thesis is to investigate knock in spark-ignition (SI) gasoline engines, more specifically, a four cylinder 2 litre four stroke Volvo engine. Since knock control systems in production vehicles have remained relatively traditional there lies an interest to investigate if improvements can be made by studying the phenomena and researching recent publications. The main goal of the thesis is to develop a closed loop knock control system that improves engine performance and fuel economy without increasing the overall knock intensities.

## 1.4 Approach

To achieve the main goal of the thesis, the following objectives will be carried out:

- Extensive research of the knock phenomena followed by further research on knock simulation techniques and knock control strategies.
- Set up a simulation environment in Simulink to analyse close loop knock control strategies.
- Develop techniques that can estimate background noise of an engine.
- Develop one or more prototype knock control softwares for engine tests.
- Quantify benefits and disadvantages compared to the traditional approach.
- Quantify fuel economy benefits when using an improved knock control strategy in a simulation environment.

# Chapter 2

## Related Research

---

This chapter contains theory regarding the knock phenomena. Different techniques used to both simulate and control knock will also be presented.

### 2.1 Knock

To understand the knock behaviour of a four stroke SI-engine, a normal combustion process needs to be explained. A normal combustion occurs when a spark plug ignites the compressed air-fuel mixture inside an engine cylinder. This results in a flame centre that grows into a turbulent flame that propagates through the cylinder in a normal velocity until it reaches the cylinder wall [1].

Knock is an abnormal combustion that originates from auto-ignition of the yet unburned end-gas (air, fuel and residual gas mixture). Heywood presents a thorough description of the knock phenomenon [1]. In short, the propagating flame ignited by the spark plug compresses the end-gas which causes a pressure and temperature increase inside the cylinder. Auto-ignition occurs when regions in the end-gas are compressed to a sufficiently high pressure for the mixture to spontaneously react. Some regions in the end-gas have a chemical composition that leads to them having a shorter time for induction, which means the time for oxidation to start. It is in these regions auto-ignition start and thus, auto-ignition does not occur uniformly in the cylinder but locally in in these so called exothermic centres [1]. In Figure 2.1, a demonstration of what happens during one of these unwanted auto-ignitions can be seen.

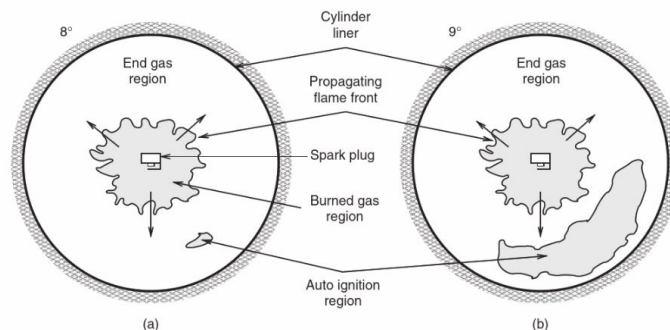


**Figure 2.1:** Top view of cylinder that illustrates the spontaneous auto-ignition of a knocking combustion. Reproduced with permission from [2].

These unwanted combustions of the end-gas occur in a period of around  $1^\circ$  CA (crank angle) and generates a shock wave, which origins from the detonation spot and bounces back and forth against the cylinder walls. The shock wave locally increases the pressure as it moves across the cylinder chamber which in turn emits an audible, pinging sound. If left uncontrolled, repeated knock cycles can cause serious damage to the engine and result in engine failure [1, 2]. These pressure oscillations can be seen in Figure 2.2.

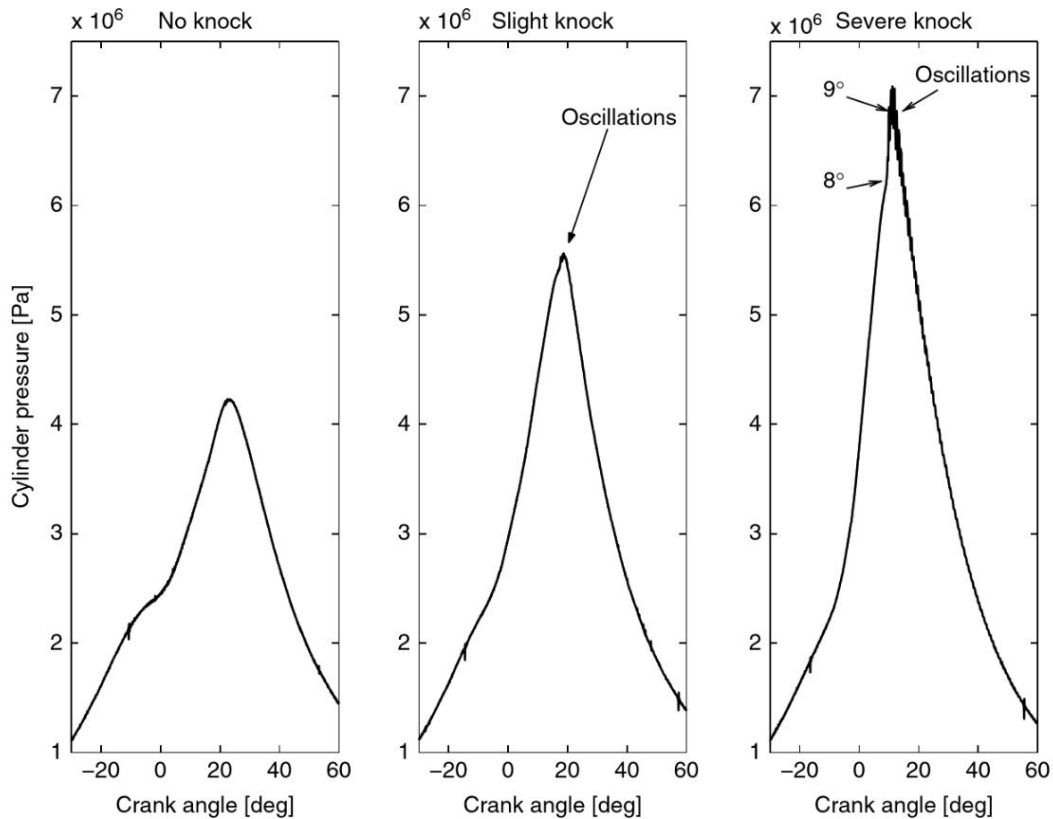


**Figure 2.2:** Pressure curve for three different combustions in the same operating condition. It illustrates the stochastic nature of the combustion as well as the pressure oscillations that is associated with the knocking sound. Reproduced with permission from [2]

## 2.2 Knock Signal Treatment and Detectability

To control knock in an SI engine, it is important to have a well performing knock detection system to properly determine if a knocking cycle has occurred. Therefore, different knock detection methods has been presented which uses a broad range of sensors ranging from microphones recording engine acoustic emissions to accelerometers measuring engine vibrations and pressure sensors measuring in-cylinder pressure [3].

The selection of a knock sensor is a race between cost and acceptable ability to detect knock. In-cylinder pressure sensors are an effective knock detector but their cost and reliability often prevents their use in production. A cheaper and more robust alternative can be achieved by using one or more accelerometers placed on the engine block. When knock combustions occur, vibrations from the pressure oscillations inside the cylinder can be measured outside the cylinder by the accelerometer to detect a knocking cycle [4]. Each cylinder can be isolated from the knock signal to determine in which cylinder the knock occurred. This makes it possible to

control spark timing individually in each cylinder which is favourable from a control perspective. Since the accelerometer measures vibrations on the engine block which is connected to several mechanically moving parts, it is susceptible to noise. To minimise its input to the detectability of knock, sensor placement and signal treatment play a big role.

By placing the accelerometer on a stiff location on the engine block, vibrations caused by knock transmit well to the sensor. Placements which react with a significant motion to vibrations are sensitive to noise. Advised placements of the accelerometers are therefore low on the engine block and axially centred [5].

To minimise noise the knock signal can be treated by introducing filters and select crank-angle windows for detection. Since the accelerometer senses vibrations on the engine block, it can be affected by vibrations caused by piston slaps and valves closing in other cylinders. To avoid these effects, a crank-angle window can be implemented around  $10^\circ$  after top dead centre (ATDC) to around  $50^\circ$  ATDC for a four-cylinder-in-line engine [4]. Frequency band filtering are commonly used to aid knock detection and analyse the signal gathered from the accelerometer. It is often tuned to pass the resonant frequencies caused by the vibrations of knocking combustions. These resonant frequencies can be found using time-frequency analysis by studying the spectral energy density of the signal from the accelerometers [6].

## 2.3 Knock Control

For ideal engine performance and efficiency, spark timing should always be set at MBT (maximum brake torque) timing. This is not realistic in all operating conditions since it will induce knock combustion events which has the ability to rapidly damage the engine. To avoid continuously repeating knock cycles, retarding the ignition timing is the mostly used control strategy in the industry today. Retarding the ignition timing from MBT affects the initiation of the flame propagation. This will lead to a lower temperature and pressure inside the cylinder and thus, decrease the probability of knock [1, 2, 7]. The disadvantage with spark retardation is its negative effect on engine performance and efficiency. Therefore, an advance towards MBT in ignition angle is desired while still maintaining an acceptable knock probability. Torque as a function of ignition angle has the typical characteristics of a second degree polynomial, see figure 2.3 [2].

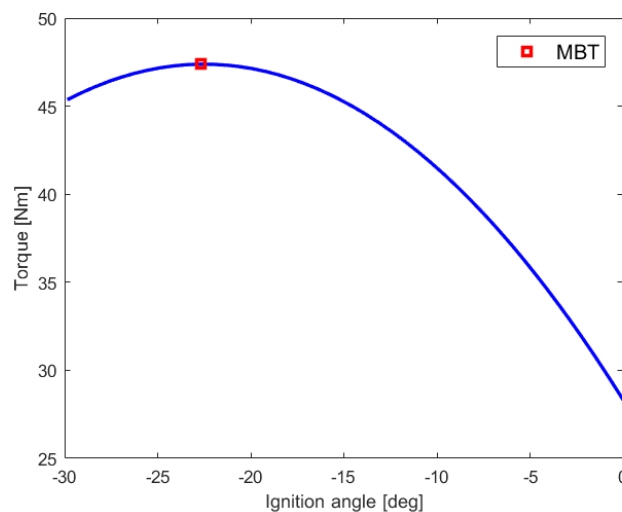


**Figure 2.3:** Curve that illustrates how torque relates to ignition angle. MBT is the maximum brake torque the engine can produce given a operating point.  $0^\circ$  represent TDC.

For operating conditions limited by knock, a knock feedback controller is initiated to control the engine knock rate to detection borderline (DBL) by controlling the ignition timing. DBL-timing is defined as an ignition timing where 1% of the combustion cycles is classified as a knock combustion [8]. Spark timing, or spark advance, is in this report defined as negative before TDC and positive after. Thus, the general spark timing control can be expressed as follows:

$$\theta_{ign} = \max(\theta_{ol}, \theta_{ol} + \Delta\theta_{fb}) \quad (2.1)$$

where  $\theta_{ol}$  is an open loop ignition control whose main purpose is to be equal to the optimal ignition timing achieved at MBT timing and  $\Delta\theta_{fb}$  is the knock feedback control compensating the spark timing in knock limited operating points [2].

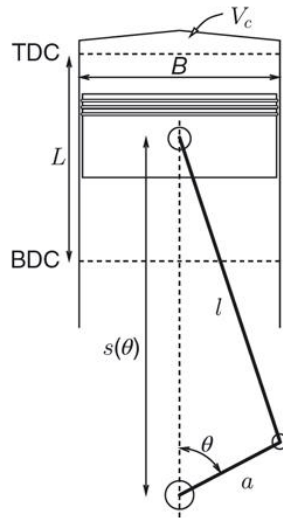


**Figure 2.4:** This is an illustration that shows relevant engine geometry from [2], reproduced with permission.

Figure 2.4 shows the geometry in a cylinder. The crank angle is here defined as positive after TDC and is used as reference for the ignition control structure shown in (2.2). In cases where relative ignition angle is shown, ignition relative to DBL-timing will instead be shown. This means that a positive value corresponds to a more advance ignition angle relative to DBL-timing.

### 2.3.1 Commonly used control algorithm

The conventional knock control strategy commonly used in production engines is a binary controller that adjusts the spark timing each combustion cycle. If a knocking cycle has been detected, the spark timing is retarded. If instead a cycle where no knock was present, the spark timing is advanced. The following equation summarises the feedback knock controller (2.2).

$$\Delta\theta_{fb}(i+1) = \Delta\theta_{fb}(i) + K_{ad} - K_{re}D_k \quad (2.2)$$

where  $K_{ad}$  is the advance gain,  $K_{re}$  the retard gain,  $D_k$  indicates if a knock cycle has been detected and  $\theta_{fb}$  holds the last state of the feedback controller. This controller is a part of the ignition control of the engine and ensures that ignition timing won't appear before the optimum spark timing that results in MBT. The advantages with this controller is that it is effective against repeated knocking cycles and its controller gains can be tuned such that a target knock probability is met [2, 7].

### 2.3.2 Statistically Based Control Algorithms

The traditional approach responds deterministic to each cycle. This means that if a knocking cycle is detected, the ignition angle is retarded for the next coming combustion and the other way around if no knock is detected the ignition angle is advanced. Therefore, the spark will be shifted back and forth around the knock limit and is in a sense "overactive". Leading to an average spark timing that on average is lower than the knocking limit. A series of publications have proposed an alternative approach that only makes spark adjustment when there is statistical evidence to do so. Peyton et al. suggested such a control algorithm that is based on cumulative summation [9]. The algorithm compares the summation of the knock events obtained data and the expected value of this summation given a desired knock probability.

Peyton et al. developed another alternative control algorithm, which later was tuned and evaluated by Thomasson et al. that uses the likelihood ratio  $L_n(k)$  [10, 11]. It is based on the fact that knock intensities are binary classified as knocking or -non knocking events. This means that the distribution of knock events are binomially distributed regardless of knock intensity. Knock intensity is further explained in section 3.1. This allows for a comparison of the probability of obtaining a given number of knocking events (if the probability of knock occurrence is truly  $p$ ), relative to the same probability calculated for the knock rate that maximises the likelihood. This means that if the likelihood ratio is close to unity, the observed data is close to the underlying probability (typically  $p = 0.01$ ). As the likelihood ratio falls closer to zero suggests that there is a mismatch and a spark adjustment should be done, the value  $L_n(k) = 0.4$  is suggested as threshold.

These new statistically based algorithms show promising result for long term steady state operation. A mean spark angle closer to DBL-timing can be achieved compared to a traditional controller if there is time to build statistical evidence without having the operating condition changed. However, questions arise whether the performance will truly be improved in a drive cycle where the engine operating point needs to be changed rather quickly and little time is given for statistical analysis.

### 2.3.3 Threshold Optimisation

Peyton et al. presented a method for optimising the knock threshold to significantly improve the closed loop performance of a conventional knock controller [12]. It is based on a stochastic view of the combustion process and aims to find a knock threshold such that it maximises the sensitivity to changes in the knock intensity distribution. This is shown to result in a closed loop controller with less dispersion in spark angle and mean spark advance that is closer to DBL. A great advantage of this method is that it only requires a re-tuning and optimisation of the already existing control strategy.

### 2.3.4 Stochastic Knock Control

Wei Luo et al., (2014) proposed a stochastic knock detection (SKD) algorithm along with a real time stochastic knock control (SKC) system. The SKC collects knock intensity information and estimates a knock intensity distribution using an FIR (finite impulse response) filter and log-normal distribution model, from which a knock factor is derived. This knock factor is then compared to a number of thresholds to generate a control action. The different thresholds are set to achieve an adaptive action that reacts more if the live-estimated distribution is far from the measured true distribution, and smaller if it is closer. This raises interest in the power of live estimation and its ability to characterise and classify the current ignition angle. This thesis aims to investigate whether the Burr Type XII distribution could be used in this manner with improved result as it is shown to more closely characterise the knock intensity.

These control and detection algorithms show prowess to increase output engine power and fuel economy by decreasing the spark dispersion and achieving a more advanced mean spark angle

when compared to the conventional controllers used in the industry today. This thesis aims to investigate and analyse these proposed control algorithms and use them as a base to develop one or a number of algorithms for improved performance.

## 2.4 Knock Intensity Distribution

The fact that knock intensity closely approximates a cyclically independent process has been shown by a number of previous studies [13, 14, 15, 16]. This means that knock intensity can be characterised completely by either its probability density function (PDF) or its cumulative distribution function (CDF). By assuming a functional form of the distribution, it is possible to store the parameters that characterise the function in lookup tables by evaluating distribution parameters as a function of engine operating condition. This provides a characterisation of the knock intensity distribution for a broad range of operation condition and can be used in order to simulate a knocking event [17]. This method of characterising knock intensity distributions is advantageous because minimal information is lost. Previous studies have sought to fit log-normal or gamma distribution models [18, 19, 20, 21]. Spelina et al. raised the importance of validation due to the fact that the result depends critically on the accuracy of the model fit and evaluated the fit of these two models with quantitative measures [22]. When compared back-to-back the log-normal distribution model was shown to perform overall better across a broad range of operating conditions. The log-normal model was also critically evaluated in its own right and in general it performed better at high and low speed but fits less well in the mid-speed region.

## 2.5 Knock Simulation

A functional knock simulation is of great value when developing, implementing and evaluating different closed loop control algorithms for knock control. There are several ways of simulating a knock event. A typical simulation environment contains a function that simulates the combustion process, followed by a simulation of the knock sensor. The signal from the simulated knock sensor is then processed in a knock detection block that calculates a knock intensity. This knock intensity is then quantified into a knock probability density function (PDF). A controller then takes this stochastic metric as input and makes controller actions in form of adjusting the spark timing. For a more in depth explanation of a typical knock simulation environment, see Peyton [17].

# Chapter 3

## Theory

---

In this chapter, relevant theory behind probability distribution fitting and statistical metrics that later will be used for the simulation environment will be presented. In depth explanations behind the knock control strategies and knock detection systems used in the thesis will also be explained.

### 3.1 Knock Detection

There are different ways to determine if a knock event occurred or not each combustion cycle. In this thesis, knock will be detected from a knock intensity signal which consists of a fraction between a knock power signal, which is a processed signal from the accelerometers on the engine block, and a noise signal. The knock power signal can be produced in different ways, see section 2.2. The noise signal is used to eliminate undesired rattling and noises caused by the surrounding environment of the accelerometers. It also normalises the signal in such a way that tolerances of the individual accelerometer output gain (mV/g) is compensated for. Knock intensity, also referred as normalised knock power, is calculated as in (3.1) where  $\psi$  is the knock power signal and  $\xi$  is the estimated background noise.

$$KI = \frac{\psi}{\xi} \quad (3.1)$$

By normalising the knock intensity, the knock threshold will be less dependent on engine operating conditions. A well functioning estimation of the noise signal is important since it affects the detectability of knock. If it estimates to low values, normal combustion cycles run the risk of being detected as knock events which will affect the knock control feedback. If it instead estimates to high values, knock events wont be registered which might end up in engine failure. Different methods to estimate noise can be used. In this thesis we propose two methods which will be further described below.

#### 3.1.1 Low-pass filter

A simple way of calculating the background noise level of the engine is to use a modified recursive average calculation of the knock power signal. Since it is not desirable to store a lot of data, a recursive average algorithm is used that only requires the previously calculated average value and the current knock power. By letting the average knocking power be denoted by  $\bar{\psi}_i$ , the previous average knocking power be  $\bar{\psi}_{i-1}$  and the current knocking power be  $\psi_i$  it is possible to formulate the following expression to estimate the background noise:

$$\bar{\xi}_i = \frac{1}{n} \sum_{i=1}^n \psi_i = \bar{\psi}_{i-1} + \frac{\psi_i - \bar{\psi}_i}{n} \quad (3.2)$$

Where  $n$  determines the impact of the next sample.

### 3.1.2 Fixed-step Background Noise Estimation

To eliminate the rising noise effects that can occur when recent knock intensity amplitudes are above or just under the knock limit, a fixed-step background noise estimation method can be used. This method does not let different knock power amplitudes affect the background in different strengths. Instead it only checks if the current knock power signal is higher or lower than the current background noise signal. The increments or decrements on the background noise is independent of the magnitude of this difference and adjusts with fixed steps. The steps lengths is a tuning parameter and controls how fast background noise can adjust whilst still being able to predict the background noise well. The estimator can be described in (3.3) where  $\xi$  is the background noise,  $\psi$  is the knock power from the accelerometers and  $k_{adv}$  determine the step size.

$$\xi(i+1) = \begin{cases} \xi(i) + k_{adj}, & \psi > \xi \\ \xi(i) - k_{adj}, & \psi < \xi \end{cases} \quad (3.3)$$

## 3.2 Stochastic Process Analysis

To get a grip of the statistical properties of knock intensities occurring in the engine cylinders each cycle and the ability to predict knock, its cyclical dependencies can be analysed. A number of previous studies have shown and stated that knock intensity is a cyclically uncorrelated process and can therefore be seen as a stochastic process [13, 14, 15, 16]. This provides evidence that knock intensity is difficult to predict and set up physical knock intensity models.

The knock intensity signal measured by the accelerometers from the engine test is shown in Figure 3.1. Although the same conditions in load, engine speed,  $(A/F)$ -ratio and ignition angle

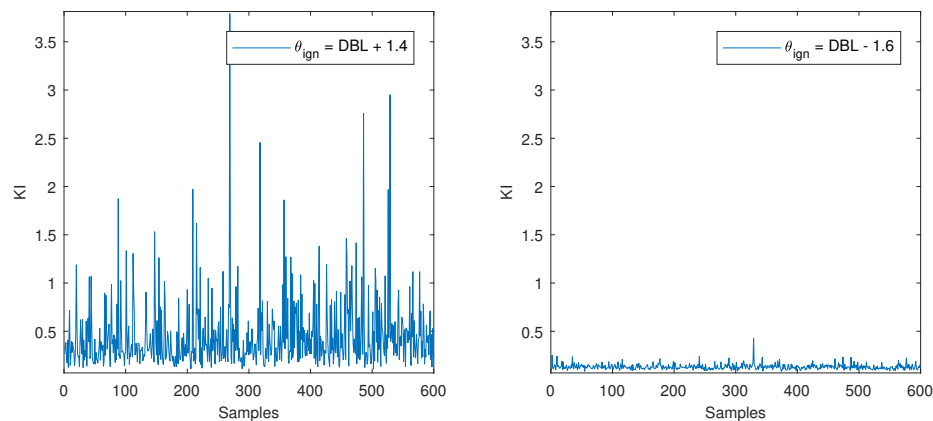


**Figure 3.1:** Knock intensity signal from two different ignition angles. The ignition angles are presented as ignition angle relative to DBL-timing were  $\theta_{ign} = 2.4$  refers to an ignition timing 2.4 CA more advanced than DBL-timing and thus, more prone to cause a knock event.

is held constant during the tests, knock intensity feedback from the accelerometers are visually noisy and unpredictable in both cases. The ignition angle dependency on knock intensity is clearly seen in Figure 3.1 were the more advanced ignition angle measures significantly higher and more frequent peaks in knock intensity.

In order to specify that knock intensity is a cyclically uncorrelated process, a scatter plot of

knock intensity for current combustion cycle against last combustion cycle can be made to examine if any linear patterns exists. A more rigorous test to study the cyclic behaviour could be done with an autocorrelation analysis. The autocorrelation analysis measures the predictability of knock intensity for a larger span of cycle lags. The autocorrelation  $R_{xx}(k)$  can be calculated using (3.4).

$$R_{xx}(k) = \frac{\sum_{i=1}^{N-k} (x_i - \bar{x})(x_{i+k} - \bar{x})}{\sum_{i=1}^N (x_i - \bar{x})^2} \quad (3.4)$$

were  $N$  is the amount of data samples in the set,  $k$  is the amount of cycle lags considered,  $\bar{x}$  is the knock intensity mean and  $x_i$  is the  $i$ :th data sample in the data set.

### 3.3 Probability Distribution Fitting

The aim of the distribution fitting is to estimate a model that is able to predict and characterise the knock intensity phenomenon, given an operation condition and a spark angle. Data reveals that large values of the knock intensity tends to be further away from the mean than small values. This is typical for a skew distribution with a positive skewness, also referred to as a 'skew distribution to the right'. For these types of distributions a number of distribution model types can be suitable. As mentioned in section 2.4 previous research suggest using a log-normal distribution. In this thesis the Burr Type XII distribution model is evaluated along with the more common log-normal distribution model.

#### 3.3.1 Burr Type XII Distribution Model

The Burr Type XII distribution is a continuous probability distribution for a non-negative random variable. It has the cumulative distribution function (CDF):

$$F(x | \alpha, c, k) = 1 - \frac{1}{\left(1 + \left(\frac{x}{\alpha}\right)^c\right)^k} \quad (3.5)$$

where  $x$  denotes the knock intensity,  $c$  and  $k$  are shape parameters and  $\alpha$  is the scale parameter. It is defined for  $\alpha > 0$ ,  $c > 0$  and  $k > 0$ . The probability density function (PDF) is given by:

$$f(x | \alpha, c, k) = \frac{\frac{kc}{\alpha} \left(\frac{x}{\alpha}\right)^{c-1}}{\left(1 + \left(\frac{x}{\alpha}\right)^c\right)^{k+1}} \quad (3.6)$$

To estimate the parameters  $\alpha$ ,  $c$  and  $k$  the Maximum Likelihood Estimation (MLE) is used. MLE is the parameters  $\hat{\theta}$  that maximises the likelihood function  $L(\theta)$  given by:

$$L(\theta) = f(x_1, x_2, \dots, x_n | \theta) \quad (3.7)$$

Where 'f' is the probability density function and ' $\theta$ ' is the parameter being estimated. In other words:

$$\hat{\theta} = \arg \max_{\theta} L(\theta) \quad (3.8)$$

is the best estimate of the parameter  $\theta$ . Since the knock intensity  $x_1, x_2, \dots, x_n \in \mathbb{R}$  are random and independent identically distributed, the likelihood function can be written as:

$$L(\theta) = \prod_{i=1}^n f(x_i | \theta) \quad (3.9)$$

By taking the gradient of the natural log of the likelihood function with respect to the parameters that are to be estimated, namely  $\alpha$ ,  $c$  and  $k$ , and setting the right hand side equal to zero. It

is possible to find the parameters  $\hat{\alpha}$ ,  $\hat{c}$  and  $\hat{k}$  that maximises the function. The log-likelihood function can be expressed as:

$$l_B(x_i|\alpha, c, k) = n \cdot \ln\left(\frac{kc}{\alpha}\right) + (c-1) \sum_{i=1}^n \ln\left(\frac{x_i}{\alpha}\right) - \sum_{i=1}^n \ln\left(1 + \left(\frac{x_i}{\alpha}\right)^c\right) - k \sum_{i=1}^n \ln(1 + (x_i + \alpha)^c) \quad (3.10)$$

In this thesis the parameters  $\hat{\alpha}$ ,  $\hat{c}$  and  $\hat{k}$  were estimated by using a non-linear programming solver. This was done in MATLAB using the solver *fminsearch*.

### 3.3.2 Log-normal Distribution Model

The log-normal distribution is a probability distribution for positive variables whose logarithm has a normal distribution. The CDF for a log-normal distribution is calculated as:

$$F_X(x | \mu, \sigma) = \frac{1}{2} \operatorname{erfc}\left(-\frac{\ln x - \mu}{\sigma\sqrt{2}}\right) \quad (3.11)$$

where  $x$  is the knock intensity,  $\mu$  and  $\sigma$  determine the shape of the distribution and *erfc* is the complementary error function expressed as:

$$\operatorname{erfc}(x) = 1 - \operatorname{erf}(x) \quad (3.12)$$

and  $\operatorname{erf}(x)$  is the error function:

$$\operatorname{erf}(x) = \int_{-x}^x e^{-t^2} dt = \frac{2}{\sqrt{\pi}} \int_0^x e^{-t^2} dt \quad (3.13)$$

The PDF of the log-normal distribution can be written as:

$$f_X(x | \mu, \sigma) = (2\pi\sigma^2)^{-1/2} \exp\left(-\frac{1}{2} \frac{(x - \mu)^2}{\sigma^2}\right) \quad (3.14)$$

To estimate the shape parameters  $\mu$  and  $\sigma$  of the log-normal model the MLE approach is used similar to how it is applied for the Burr type XII model. The likelihood function is given by

$$\begin{aligned} L(x_1, x_2, \dots, x_n | \mu, \sigma) &= f(x_1, \dots, x_n | \mu, \sigma) = \prod_{i=1}^n f(x_i | \mu, \sigma) \\ &= (2\pi\sigma^2)^{-n/2} \exp\left(-\frac{1}{2\sigma^2} \sum_{i=1}^n (x_i - \mu)^2\right) \end{aligned} \quad (3.15)$$

By taking the partial derivative of the natural logarithm of the likelihood function with respect to  $\mu$  and  $\sigma^2$  and setting the right hand side equal to zero it is possible to find the  $\hat{\mu}$  and  $\hat{\sigma}^2$  that maximises the log-likelihood function. The log-likelihood function is

$$l(x_1, x_2, \dots, x_n | \mu, \sigma^2) = -\frac{n}{2} \ln(2\pi) - \frac{n}{2} \ln(\sigma^2) - \frac{1}{2\sigma^2} \sum_{i=1}^n (x_i - \mu)^2 \quad (3.16)$$

The resulting parameters  $\hat{\mu}$  and  $\hat{\sigma}$  that maximises the likelihood function (3.14) is given by the following expressions:

$$\begin{aligned} \hat{\mu} &= \frac{\sum_{i=1}^n \ln(x_i)}{n} \\ \hat{\sigma}^2 &= \frac{\sum_{i=1}^n \left(\ln(x_i) - \frac{\sum_{i=1}^n \ln(x_i)}{n}\right)^2}{n} \end{aligned} \quad (3.17)$$

### 3.3.3 Knock Intensity Error at the 95th Percentile

A critical measure is to quantify the modelling error at the tail of the distribution, in particular for closed loop control systems. This is due to the fact that conventional and as well as most suggested controllers in section 2.3 act on the binomially classified knock events that occur at high values of knock intensities (in the tail of the distribution). To quantify how well the model describes the knock intensity at this critical portion, the error  $Err(x_{0.95})$  in the 95th percentile knock intensity have been used broadly, see [20, 22]. It is expressed according to:

$$Err(x_{0.95}) = \left| F^{-1}(0.95) - \hat{F}^{-1}(0.95) \right| \quad (3.18)$$

Where  $F^{-1}$  is the inverse of the CDF calculated for the data and  $\hat{F}^{-1}$  is the inverse of the estimated model CDF. Spelina et al. suggest using the percentage intensity error since these errors depend on the gain of the sensor [22]. The more appropriate suggested metric of the percentage intensity error is simply calculated as:

$$\%Err(x_{0.95}) = \frac{\left| F^{-1}(0.95) - \hat{F}^{-1}(0.95) \right|}{F^{-1}(0.95)} \times 100 \quad (3.19)$$

### 3.3.4 Probability Error at Knock Event

By expressing the probability error in vicinity of the threshold knock intensity it is possible to get a measure of how wrong the PDF is at this point. It is common practice to set the borderline knock limit to where one percent of the combustions are regarded as knocking. Thus the probability error at knocking event can be written as:

$$Err(p_{0.01}) = |p - \hat{p}| = \left| f(x_{th}) - \hat{f}(x_{th}, \theta) \right| \quad (3.20)$$

Where  $x_{th}$  is defined as the knock intensity threshold and  $\theta$  represent the estimated model parameters.

### 3.3.5 Kolmogrov-Smirnov Test Statistic

A fit for the distribution as a whole can be found testing how well the empirical CDF from measured data and model conform. This can be done with a Kolmogorov-Smirnov (KS) test statistic. It provides a rigorous method for testing whether the distribution is consistent with a complete set of data by rejecting the hypothesis of the specified distribution at the significance level  $\alpha$  if the test statistic  $D$  exceeds a critical value. The critical value can be found in tables and are dependent on desired significance level as well as the amount of gathered data points in the set. The test statistic itself (often referred to as KS distance) is the supremum of the absolute error between the modelled CDF and the CDF calculated from data according to (3.21). [23]

$$D = \sup_x \left| F(x) - \hat{F}(x, \theta) \right| \quad (3.21)$$

Where  $x$  is the measured knock intensity and  $\theta$  is the estimated model parameters of the specified distribution CDF function.

### 3.4 Knock control

The overall goal of any knock controller is to avoid potentially damaging or NVH (noise vibration harshness)-inducing knocking events. Under this chapter, some of the knock control strategies presented in chapter 2.3 which will be implemented and tuned in the simulation environment will be further described. The knock controllers will result in the feedback part  $\Delta\theta_{fb}$  of the ignition timing controller in (2.2).

#### 3.4.1 Conventional Controller

A common knock controller widely used in the automotive industry today is here named as "conventional knock controller". It's a robust and simple deterministic control strategy that conversely advances the spark timing if no knock is detected and aggressively retards the spark timing if a knock is detected. This control algorithm is therefore often referred to as a "slow advance fast retard" strategy. The controller can be summarised by following equation:

$$\theta_{ign}(i) = \begin{cases} \theta_{ign}(i-1) + k_{adv} & \text{Non knocking cycle} \\ \theta_{ign}(i-1) - k_{ret} & \text{Knocking cycle} \end{cases} \quad (3.22)$$

where  $k_{adv}$  and  $k_{ret}$  is controller gains determining ignition angle advance and retard respectively. These parameters can be tuned to match a desired knock probability by evaluating following expression:

$$k_{adv}(1-p) = k_{ret}p \quad (3.23)$$

Which can be rewritten as

$$k_{adv} = k_{ret} \frac{p}{1-p} \quad (3.24)$$

where  $p$  is the desired knock probability. The output of the conventional knock controller for an operating point, limited by knock, can be seen in Figure 3.2.

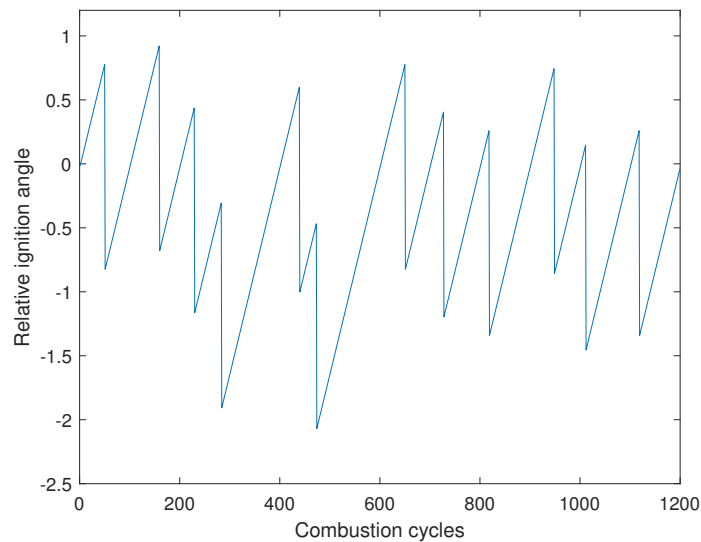


**Figure 3.2:** Characteristic behaviour of a conventional knock controller.

### 3.4.2 Cumulative Summation Based Control

A cumulative summation based knock controller has the advantage that it takes into account that knock is a stochastic process. If a knock is detected, it only reacts and adjusts the spark timing if a specified threshold is breached. The controller builds its own statistics each cycle without the need of large data buffers that saves data from previous cycles. Instead two variables are updated simultaneously in each combustion cycle. These variables are a reference knock probability ( $EK$ ) and a live knock probability ( $KP$ ) which strives to be equal to the reference to achieve DBL spark timing. The reference knock probability adds the desired probability each combustion cycle and will then increase linearly each cycle based on the given probability. The live knock probability is a knock counter and will instead behold the "real" knock probability for the current operating point. If a knock is detected, this variable is added by 1 and cycles without knock its held constant. This knock probability is summarised as

$$KP(i+1) = \begin{cases} KP(i) & \text{Non knocking cycle} \\ KP(i) + 1 & \text{Knocking cycle} \end{cases} \quad (3.25)$$

---

**Algorithm 1** Pseudo code for the cumulative summation controller executing each combustion event

---

```
1: increment  $EK$  by  $p_{des}$ 
2: if knocking then
3:   increment  $KP$  by 1
4: end if
5: if  $KP > (EK + high_{thr})$  then
6:   retard spark angle
7:   set  $EK = 0$ 
8:   set  $KP = 0$ 
9: else if  $KP < (EK - low_{thr})$  then
10:  increase spark angle
11:  set  $EK = 0$ 
12:  set  $KP = 0$ 
13: end if
```

---

A region around the desired knock probability is created by upper and lower thresholds from the desired knock probability. If the actual knock probability reaches outside this region, a spark adjustment will be made and both the desired and the actual knock probabilities will be reset. If the upper threshold is met, knock probability is too large and a retardation in ignition angle will be made. if the lower threshold is met we have a ignition angle that is unnecessarily retarded and should therefore be advanced. A simple algorithm for this knock controller is seen in Algorithm 1. Figure 3.3 graphically shows how the controller is supposed to act. The difference is that  $EK$  were not reset to zero when the control boundaries were breached and instead  $KP$  were set equal to  $EK$  for presentation purpose. The linearly increasing line is dependent on the desired probability and the red line, describing  $KP$ , is calculated by the expression

$KP = \frac{\text{detected knocks}}{\text{combustion cycles}}$ . To further develop this control strategy, its controller gains can be scaled with the likelihood ratio of knock described in section 3.4.3 with the factor  $(1 - Ln)$ , were  $Ln$  is the likelihood ratio. Thus, the controller must be convinced by two statistical metrics to perform larger steps in ignition angle. Another add-on to speed up the controller is to decrease the length to the lower boundary in the case of repeating spark advances. When the upper boundary later is breached due to frequently repeating knocking cycles, the lower boundary is reset to its normal value. this would speed up the controller to find DBL-ignition in case of an initially retarded spark angle.

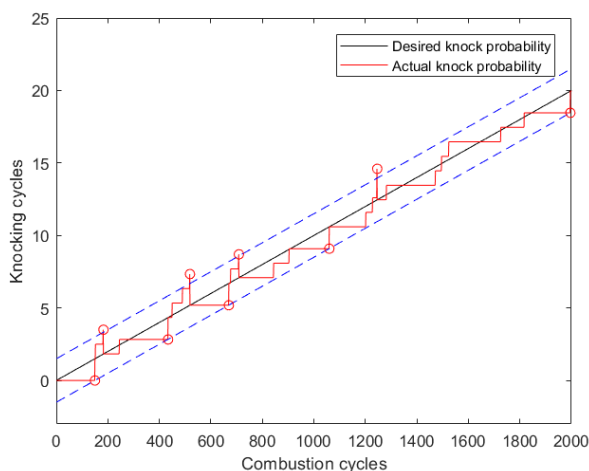


**Figure 3.3:** A cumulative summation knock controller with desired knock probability  $p = 1\%$ . The dashed lines visualises the upper and lower boundaries of the controller and the circles are plotted if a spark adjustment were made.

### 3.4.3 Likelihood Based Controller

As already mentioned in section 2.3, the resulting knock intensity from each combustion is either classified as knock or non-knocking in case it passes a certain threshold. This means that the knocking events are defined as binomially distributed regardless of knocking intensity and has the probability mass function

$$p_n(k) = \binom{n}{k} p^k (1-p)^{n-k} \quad (3.26)$$

This evokes thoughts about using this in a control strategy. However, for control purposes this calculated probability unfortunately has very little usefulness. For instance, if the target knock rate is  $p = 1\%$  and only one knock has been observed during the last 150 cycles the probability of that occurrence is  $p_{150}(1) = 33.56\%$ . Only one knock during 150 combustions implies a spark advance could be done, however the probability of observing one knock during 100 cycles  $p_{100}(1) = 36.97\%$  is very similar. A more useful measure is a likelihood ratio where the probability of a outcome with underlying probability of  $p = 1\%$  is compared to the knock rate  $p_{max} = k/n$  that maximises the likelihood.

$$L_n(k) = \frac{p^k (1-p)^{n-k}}{p_{max}^k (1-p_{max})^{n-k}} \quad (3.27)$$

The likelihood ratio will be close to unity if the spark advance is such that knocking combustions occur at roughly 1% of the combustions, thus implying that the actual knock probability is close to the target knock probability. A likelihood ratio that falls to zero suggests that a spark adjustment should be done. This property gives a good measure of how far off the current spark adjustment is compared to DBL and can thus be used to scale the gain parameters with the factor  $(1 - Ln)$ .

Since the control algorithm relies on statistical evidence to make advance actions poor controller performance is to be expected when the spark angle is unnecessarily retarded. This provoked a fast forward improvement has been proposed by Peyton et al. and was later evaluated and tuned by Thomasson et al. [10, 11]. This fast forward algorithm has been adopted. An alteration has been made to the proposed method on making the performance robust for longer steady state operation. The pseudo code for the controller is described in algorithm 2. The fast forward part is executed by adding non-knocking cycles as a function of previously consecutive spark advances. This is done through the cycle count after spark advance ( $k0$ ) vector with the spark

advance counter (SAC). During long steady state operation without spark adjustment a large number of knocking events needs to occur to lower the likelihood-ratio enough to trigger a spark retardation. To prevent this, a limit is set on the number of knocking events and the number of non-knocking cycles are reduced (see line 9-12 in algorithm 2). Figure 3.4 illustrates likelihood-ratio curves for different amount of knocking events and figure 3.5 shows the fast forward part of the the controller from simulation and figure 3.6 shows the fast retardation response.

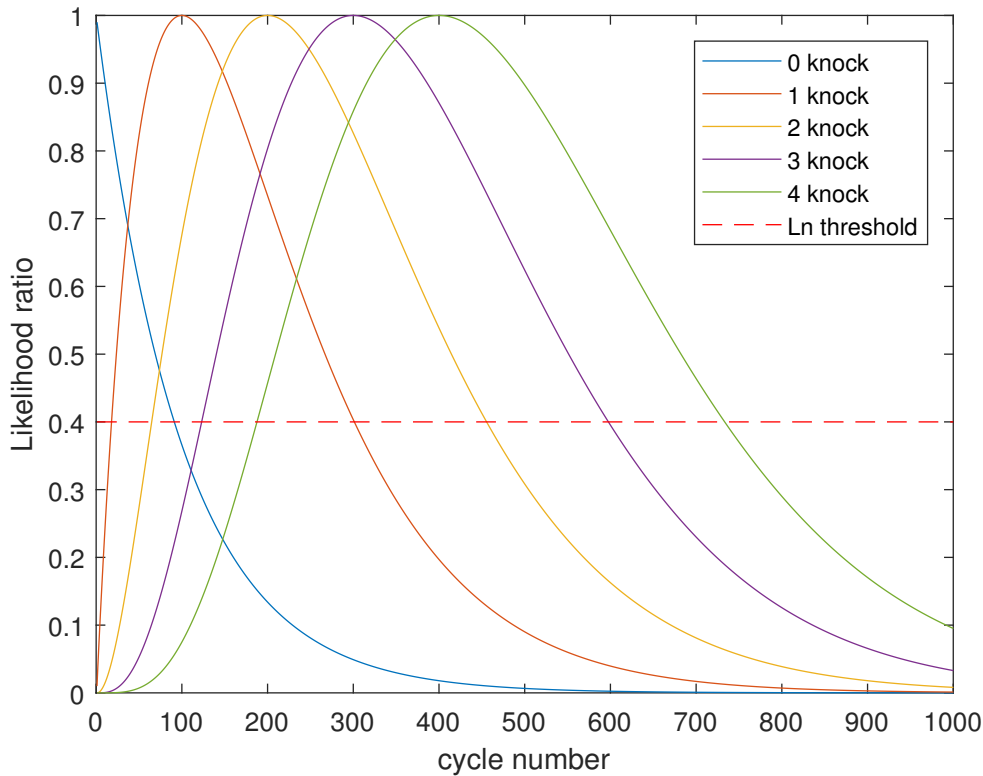


**Figure 3.4:** Likelihood ratio as function of cycle number for different amount of knocking events. For 1 knock event unity is at 100 cycles since the target knock rate is set to 1 %. If the likelihood-ratio falls below the threshold at 0.4 a action will be triggered.

The live likelihood ratio will follow one of the curves shown in figure 3.4 depending on the number of knock events. If for instance two knocking events has occurred in 120 cycles, the likelihood-ratio would be around 0.7 (yellow curve). If the following cycle would have been a knock event, the ratio will take the value around 0.35. This would then trigger a spark retard since it is below the specified threshold. If instead 2 knocking events has occurred and the cycle count surpasses 455 cycles, a spark advance will be triggered.

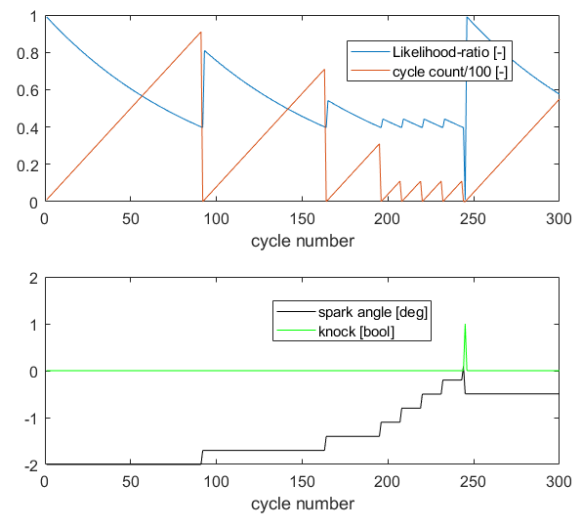


**Figure 3.5:** Demonstration of the fast forward part of the Likelihood-based controller algorithm for 2000 rpm 500 mg/stk condition when the initial spark is unnecessarily retarded (from simulation). When advances occurs the SAC and  $k_0$  will decrease the amount of cycles required to make an advance. Since this keeps the Ln-ratio low the algorithm will respond quickly to a knock.

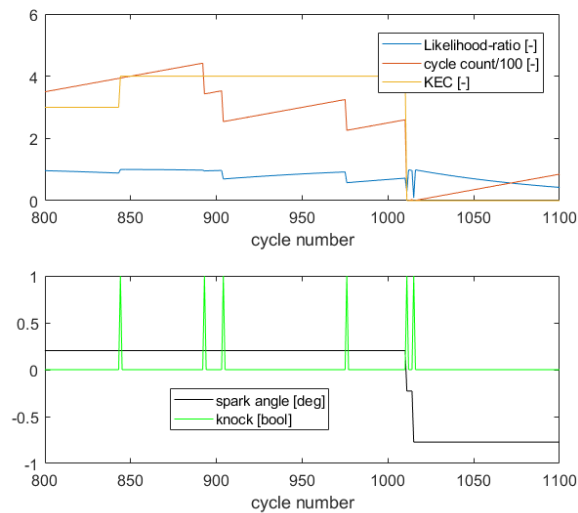


**Figure 3.6:** Demonstration of the fast retard response part of the Likelihood-based controller algorithm for 2000 rpm 500 mg/stk condition when the DBL is shifted backwards by 1 deg after 1000 cycles. The algorithm keeps KEC at 4 and subtracts cycles from the likelihood calculation which results in a lowered ratio that triggers a spark retardation.

---

**Algorithm 2** Pseudo code for the Likelihood controller

---

```
1: Initialise Knock Event Counter  $KEC=0$ ;  
2: Initialise Spark Advance Counter  $SAC = 0$ ;  
3: Initialise cycle count  $n = 0$ ;  
4: Initialise Cycle count after spark advance  $k0 = \{0, 20, 40, 60\}$   
5:  $Ln_{thr} = 0.4$   
6: if Knock then  
7:    $KEC = KEC+1$ ;  
8:    $SAC = 0$ ;  
9:   if  $KEC > 4$  then  
10:     $KEC = 4$ ;  
11:     $n = n-100$ ;  
12:   end if  
13: end if  
14: if  $SAC \neq 0$  then  
15:    $P_{max} = KEC/(n + k0(SAC))$ ;  
16: else  
17:    $P_{max} = KEC/n$ ;  
18: end if  
19:  $Ln = L(n+k0(SAC))$ ;  
20: if  $Ln < Ln_{thr}$  then  
21:   if  $P_{max} < target\ rate$  then  
22:      $SA = k_{adv}(1 - Ln)$ ;  
23:      $SAC = \min(SAC + 1, 3)$ ;  
24:   else  
25:      $SA = k_{ret}(1 - Ln)$ ;  
26:      $SAC = 0$ ;  
27:   end if  
28:    $KEC = 0$ ;  
29:    $n=0$ ;  
30: end if
```

---

### 3.4.4 Threshold optimisation

The aim of the knock control algorithm is to prevent engine damage and to reduce the audible pinging noise that occurs when knock intensity levels are too high. Thus, knock intensities are usually classified as knocking or non-knocking by some set threshold. This classification is then used in the feedback loop to make spark adjustments. There exists different strategies to define a appropriate threshold. The typical method is to set a threshold such that 1 % – 4 % are classified as knocking under borderline conditions. Figure 3.7 shows how knocking probability changes for different scales of knock threshold.

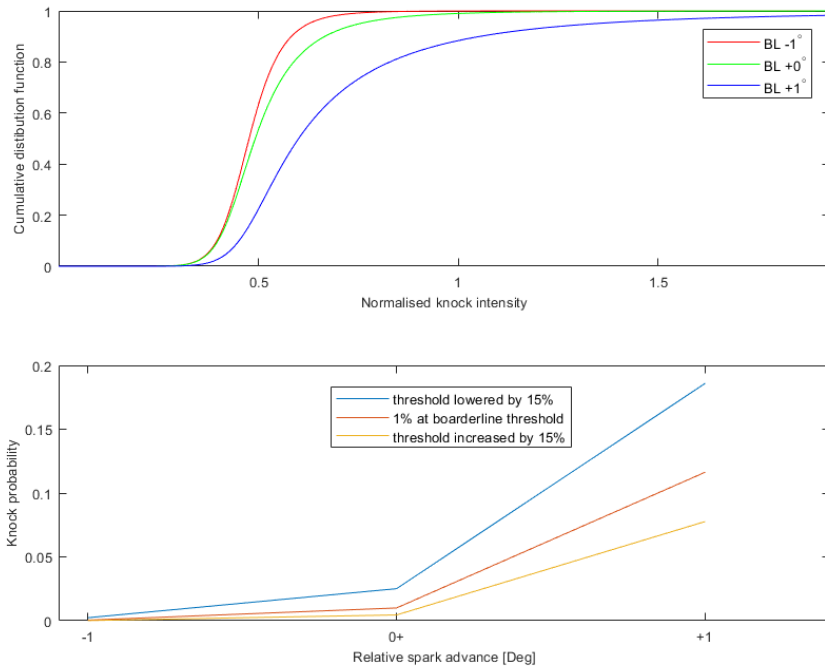


**Figure 3.7:** The figure shows CDF estimates to measuring data for operation condition 2000 rpm and 500 mg/stk and knock probability as a function of spark advance.

Peyton et al. proposed a different approach when determining a appropriate threshold level [12]. The proposed method is to use a feedback signal that from a control perspective would be optimal. Since the controller aims to keep the spark advance as close as possible to the set point target spark angle, an optimal feedback signal to the controller would be the signal that is most sensitive to deviations to this set point target. In this case the set target point is the knocking probability at borderline condition and the deviation is the change in knock probability. Peyton et al. therefor suggest the sensitivity that should be maximised to be calculated as

$$s = \left( \frac{1}{\sqrt{p(\theta)(1-p(\theta))}} \frac{\partial}{\partial \theta} \right) \Bigg|_{\theta=BL} \quad (3.28)$$

Where  $p(\theta)$  is the knocking probability as function of spark angle given a knock threshold. The  $\sqrt{p(\theta)(1-p(\theta))}$  factor is the standard deviation of the number of knocking events in any fixed number of cycles and is used to normalise the function. Since a 1 % deviation is "large" if the target knock rate itself is 1 %. The authors suggest adding a small constant to the denominator of expression (3.28). Also, since no analytic expression for  $p(\theta)$  is available a numeric derivative

based approximation of  $\frac{\partial}{\partial \theta}$  is used. The resulting expression for the sensitivity function is:

$$s \approx \frac{p(\theta_{BL+1}) - p(\theta_{BL-1})}{2 \left( 0.1 + \sqrt{p(\theta)(1 - p(\theta))} \right)} \quad (3.29)$$

By evaluating this sensitivity criterion as function of different scales of knock threshold, it is possible to find the optimal threshold for feedback purposes. The optimal threshold that maximises the sensitivity criterion will then behold the optimal threshold scale. The desired weak knockrate that corresponds to the optimal threshold can be found from the knock intensity CDF at DBL-timing by the intersection of the CDF and the optimised threshold.

The optimised threshold can be used on knock controllers that utilises a desired knock probability by alternating the previously knock probability with the desired weak knock rate given at DBL-timing of the optimised threshold.

### 3.4.5 Cumulative summation based knock controller with likelihood-scaled controller gain and optimised threshold

By fusing together the knock control strategies earlier stated in this chapter, a lot of different knock controllers can be created. One of which will be presented in this report. It is based on the cumulative summation method for determining when a spark adjustment should be executed whilst optimising the threshold and scaling the adjustment steps with the likelihood function described in 3.4.3. This results in a controller that is treating knock as a stochastic process by comparing its cumulative summation variables, a more sensitive controller due to the optimised threshold which acts on weak knock events and more precise spark adjustments due to the likelihood scaled controller gains.

As discussed in section 5.3.1, the optimal threshold for the current operating condition can be calculated using a sensitivity function to instead aim at a desired weak knock rate. This means that the expected knock rate  $p_{des}$  will be changed and the slope of the slope of the variable EK will be altered.

### 3.4.6 Live estimation of Burr Type XII distribution controller

This controller type requires a lot of knowledge about the knock intensity distribution in each operating point it is supposed to be used for to perform well. By collecting data of a spark sweep around DBL timing, it is possible to estimate well fitted distributions for the operating point. DBL-timing can be found by analysing the knock rate from the spark sweep and thus, the burr type XII parameters at DBL-timing of the current operating point can be calculated. With this knock intensity distribution knowledge, it is possible to control the spark timing by observing the live Burr Type XII parameters since its parameter value for DBL-timing is known from the spark sweep experiment.

Based on a number of knock intensity samples, a Burr Type XII distribution is estimated using the maximum likelihood estimation. The number of samples can be chosen in a number of ways. By increasing the number of samples used to estimate the distribution results in more precise estimations. The drawback however is that it increases the time it takes to evaluate and in a case were a spark adjustment is desired, a control action will be delayed. The sample size can be chosen by estimating CDFs of different sample sizes and calculate a knock factor as in [24] for each estimation. By calculating the variance of the knock factors tells how well the distributions coincide. A high variance would mean less exact results and thus, as low variance as possible is desired.

When the distribution parameters are estimated they are compared to the DBL-timing parameters and ignition angle can be adjusted based on the difference between these parameters.

# Chapter 4

## Simulation Environment

---

In this chapter the development of the knock intensity simulation environment will be presented. Since the simulation environment will be statistically based from real engine data, this chapter will begin with a statistical analysis section of gathered data followed by introducing the results into a simulation environment.

### 4.1 Overview of the simulation environment

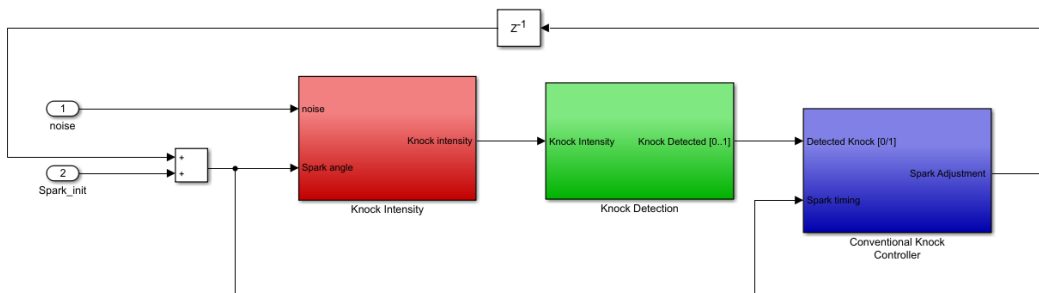


**Figure 4.1:** Capture of the simulation environment created in Simulink.

An overview of the simulation environments are shown in Figure 4.1. In the red subsystem knock intensity is produced from an ignition angle and introduced noise input. The noise input shifts DBL position either in advance ignition angle direction or retard direction without affecting the ignition angle in the controller loop. This is an effective tool in order to test the controllers transient response or ability to find DBL in case it shifts position. Figure 4.2 captures how the knock intensity block signals are used to generate a knock intensity signal. After a knock intensity is produced, it will be characterised as a knocking or non-knocking event from the green subsystem by a knock threshold set manually. Figure 4.3 shows this simple detection structure. In case of threshold optimisation controller is used, the threshold characterising weak knock events will be scaled from the knock threshold used. The blue box contains the controller that is to be tested. The controller adjusts the ignition angle in the next combustion cycle (if required) by adding or subtracting the calculated adjustment to the previous ignition angle. The new ignition angle is then fed back to the knock intensity block to generate a new knock intensity based on the distribution of that ignition angle. The method is evaluated in section 5.1 by comparing the knock intensities generated by the simulation model to the ones measured in tests. Figure 4.4 captures the simple structure of the conventional controller.

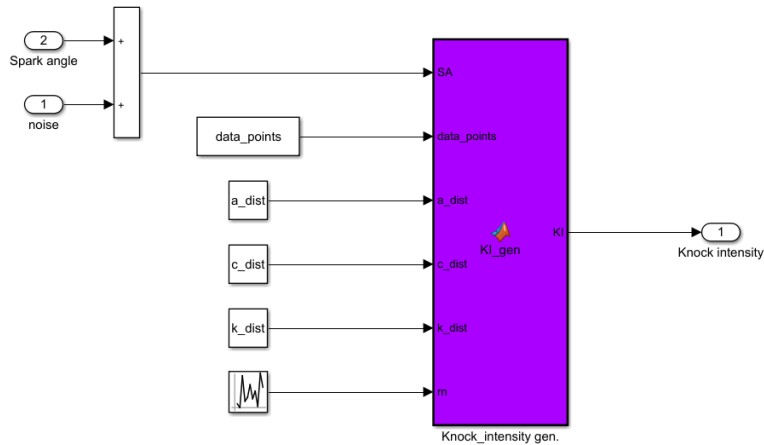


**Figure 4.2:** Capture of the simulation environment inside the Knock Intensity block. The spark and noise are input from the environment. *rn* is a random number generator and the rest are operating dependant constants loaded with initialising scripts.

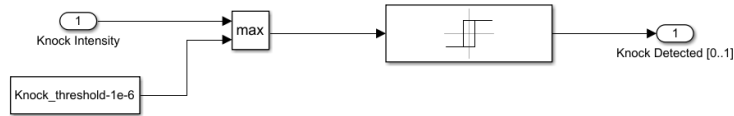


**Figure 4.3:** Knock detection structure.

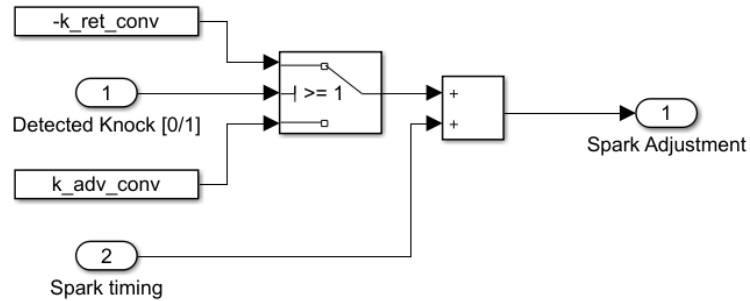


**Figure 4.4:** Conventional controller structure in the simulation environment.

## 4.2 Simulation of Knock Intensity

Lonari et al. showed that the functional form of the distribution can be parametrically characterised by a log-normal curve [24]. By calculating a normal mean and variance of the measured knock intensity it is possible to derive the log-normal mean and variance.

The knock intensity simulation environment in this thesis is instead based on the Burr Type XII distribution. This distribution, discussed in chapter 3.3.1, is chosen instead of a log-normal distribution since it is shown to characterise knock intensity more precisely. Figure 4.5 shows how the distribution of knock intensity changes with ignition timing for a fixed operating condition. These data sets with fixed ignition angle are used when fitting the distribution models to data. The data is collected from real-life testing where the ignition angle was kept constant at a desired value. The air-fuel ratio during the measurements were controlled such that a fixed  $\lambda$  of  $\lambda = 1$  was aimed at during the measurements. In each operating point data were measured, the Burr Type XII distribution parameters  $\alpha$ ,  $c$  and  $k$  are mapped up using maximum

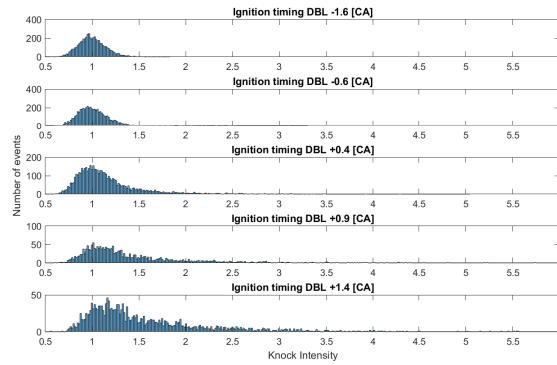


**Figure 4.5:** Histogram showing how the knock intensities are distributed for different ignition timings. The data was collected at operating condition 2000rpm 500mgair/stroke. A more advanced ignition angle leads to a wider spread and has a higher probability of experiencing higher knocking intensities.

likelihood estimation shown in section 3.3.1. If an ignition angle between two measured points is to be evaluated, their parameters will be calculated by interpolating between the points in the map. This can be seen in Figure 4.6 where the probability density functions for different ignition angles are shown. The data were gathered for the operating condition 2000 rpm, 500mg air/stk and the air-fuel ratio was controlled such that  $\lambda = 1$  was achieved. The ignition angles  $\theta_{ign} = DBL + \{-1.6, -0.6, 0.4, 0.9, 1.4\}$  shown in the figure were calculated from measured data points whilst  $\theta_{ign} = DBL + \{-1.1, 0.1, 1.9\}$  were calculated by interpolation between the closest ignition angle parameters of the burr distribution.

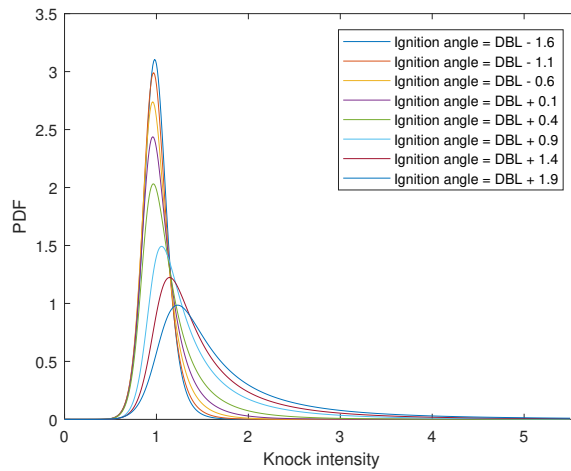


**Figure 4.6:** Probability density functions estimated using the Burr Type XII model for different ignition timings. The ignition angles are defined as relative to DBL-timing. In this case, a positive ignition angle means an ignition timing more advanced than DBL-timing. As can be seen, more advanced ignition timings results in both more and higher knock intensities.

When the Burr Type XII parameters has been calculated for the actual ignition angle, a knock intensity is generated from the distribution through its inverse cumulative distribution function using (4.1). The CDFs for the ignition angles  $\theta_{ign} = DBL + \{-1.6, -0.6, 0.4, 0.9, 1.4\}$  from measured data can be seen in Figure 4.7. The parameter  $X$  is a uniformly distributed random

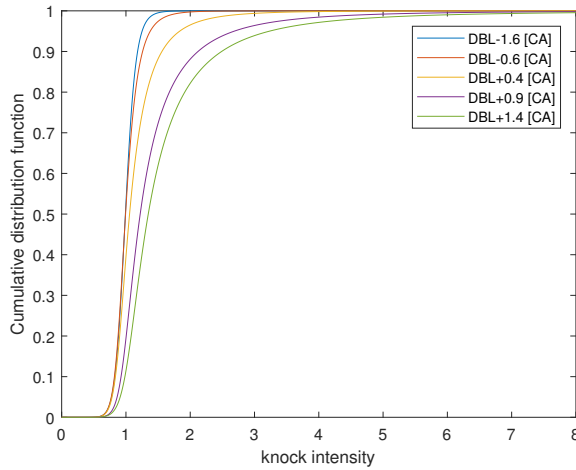


**Figure 4.7:** Cumulative distribution function calculated from measured data using the Burr Type XII model. The ignition angles are defined as relative to DBL-timing. In this case, a positive ignition angle means an ignition timing more advanced than DBL-timing. As can be seen, more advanced ignition timings results in both more and higher knock intensities.

variable with values ranging between 0 and 1.

$$KI(X|\alpha, c, k) = \alpha((1 - X)^{\frac{1}{-k}} - 1)^{\frac{1}{c}} \quad (4.1)$$

In Figure 4.8 the inverse of the Burr Type XII CDF is shown for the case were DBL ignition angle is reached and 1% knock is achieved. Since it is equally possible to draw each random variable  $X$ , the output knock intensity from (4.1) will generate knock intensities such that the desired probability density function is attained.

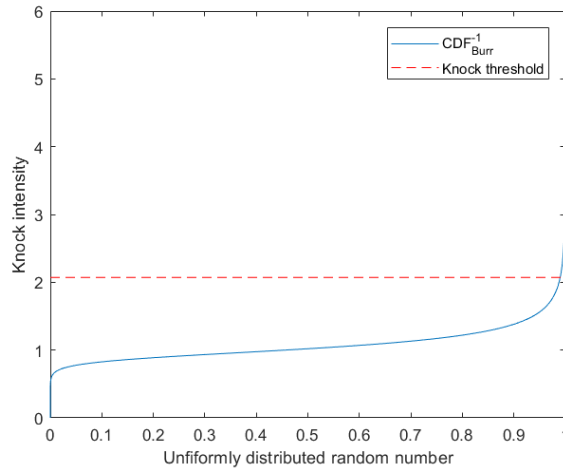


**Figure 4.8:** The solid blue line is the inverse of the cumulative distributing function. The dashed red line is the knock thresholded value. By examining the figure one can see that this threshold would lead to 1 % knock since it intersects with the CDF inverse at the value 0.99.

# Chapter 5

## Results

---

In this chapter, the results from the statistical analysis of knock intensity will be presented followed by the results from the knock controllers and noise estimators.

### 5.1 Stochastic analysis

A stochastic analysis was performed to investigate if there exists any correlation patterns of the knock intensity signal. In Figure 5.1 a scatter plot of knock intensity for current combustion cycle against last combustion cycle is shown. The scatter plot shows little to none cyclic behaviour patterns in the knock intensity signal for the  $\theta_{ign} = DBL + 1.4$  case and for the  $\theta_{ign} = DBL - 1.6$  case no such patterns can be seen. The scatter plot does not account for cycle lags larger than

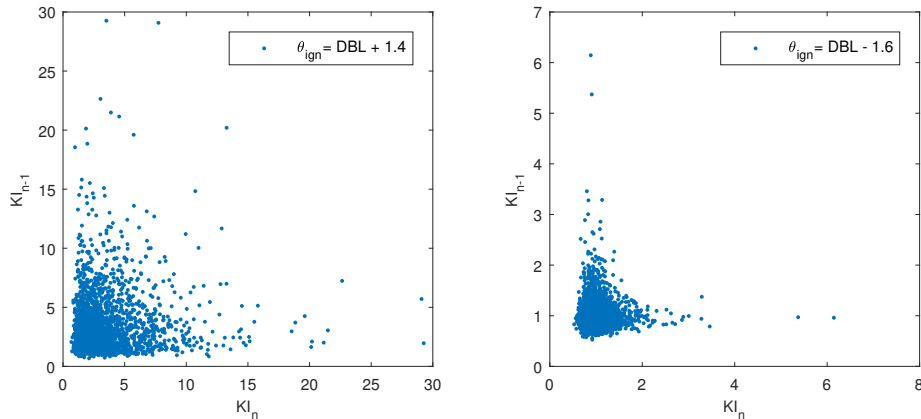


**Figure 5.1:** Scatter plot of knock intensity at cycle  $k$  vs cycle  $k-1$ . No linearity shown in either case which would indicate that a knock cycle could be expected given an earlier knocking cycle. The ignition angle  $\theta_{ign}$  is relative ignition angle from DBL where a positive value means a more advanced ignition angle.

one cycle and therefore a more comprehensive test of the stochastic nature of knock intensity is desired. An autocorrelation analysis was therefore made with a cycle lag of up to 10. The autocorrelation seen in Figure 5.2 shows that all cycle lags falls inside the 95% confidence interval except a cycle lag of 5 which is just outside the borders for the case with relative spark advance  $\theta = DBL - 1.6$ . With the more advanced  $\theta = DBL + 1.4$  data set, cycle lag of 1 and 8 falls

outside the intervals but again, just slightly above the 95% confidence interval. Both cases strengthens the hypothesis that knock intensity is a cyclically uncorrelated process.

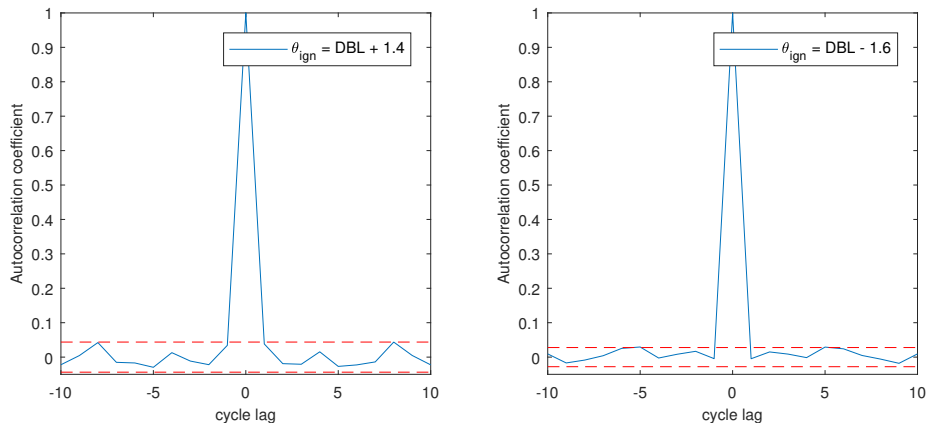


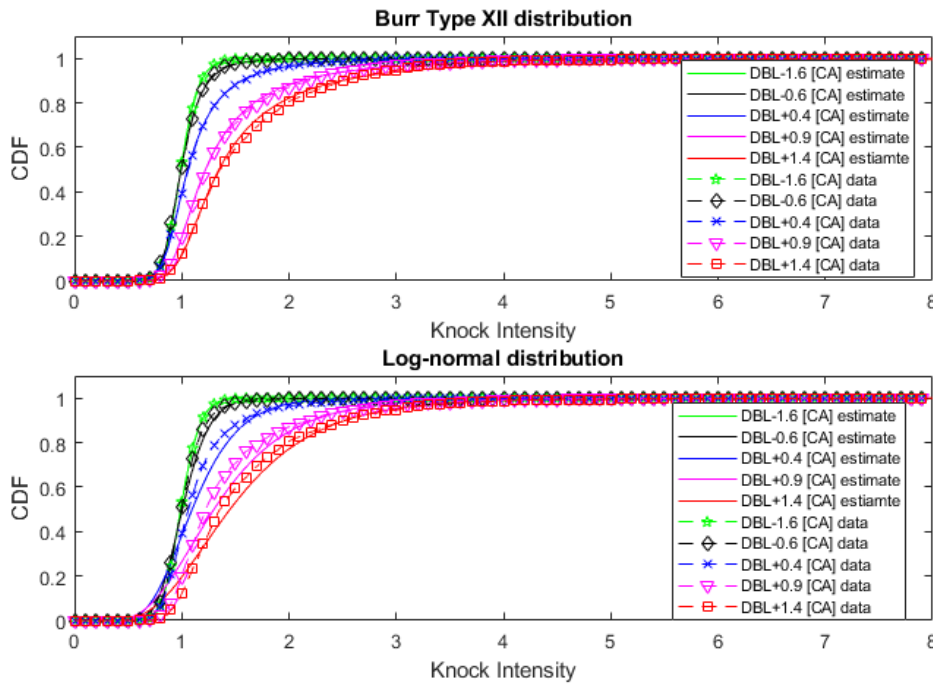
**Figure 5.2:** Auto-correlation analysis of knock intensity with cycle lag up to 10 samples along with a dashed line showing the 95% confidence interval borders. No correlation can be seen in either the advanced or retarded ignition angle since the autocorrelation lies within the confidence interval borders.

## 5.2 Distribution Model Evaluation

To evaluate the "goodness of fit" of the distribution models various methods can be used. To put Burr Type XII distribution model into context it is evaluated along side with the log-normal distribution model. The Kolmogorov-Smirnov test statistic is used to determine whether the distribution model should be rejected or not at the significance level  $\alpha$ . However, it could be argued that the KS statistic is inappropriate in knock application since it is only the probability error in the vicinity of the threshold on knock that affects the overall knocking probability. Therefore the knock probability error at threshold level as well as knock intensity error at the 95th percentile is used to evaluate the distribution estimation.

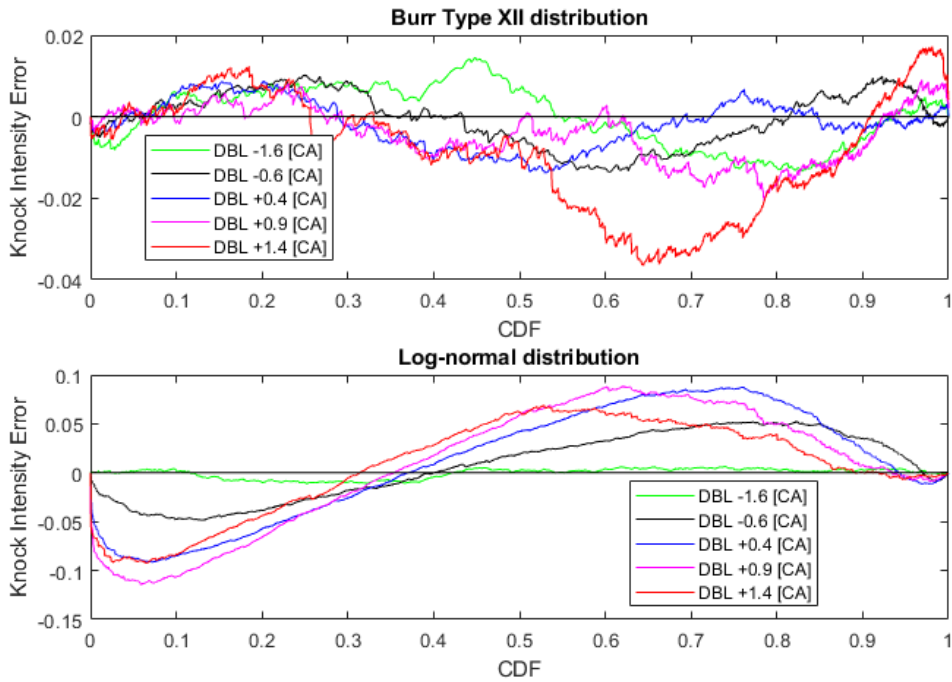
### 5.2.1 Knock Intensity Error at the 95th Percentile

Figure 5.3 shows the Burr Type XII distribution model and Log-normal distribution model CDF estimate and the CDF calculated from measurement data. Generally, the Burr model can be seen to have a better fit, especially for the more advanced ignition angles. The differences between the CDF curves can be viewed in figure 5.4 as knock intensity error. The knock intensity error elucidates what is seen in Figure 5.3. The percentage knock intensity error according to (3.19)



**Figure 5.3:** Knock intensity CDF and the corresponding Burr Type XII and Log-normal distribution estimates. Data was measured at operating condition 2000 rpm and 500 mg/stk.

can be seen in Figure 5.5. By examining this figure along side with figure 5.4 one can see that overall the Burr Type XII model has a better fit. However, at the tail of the distribution for the data set  $DBL + 0.9$  [CA] and  $DBL + 1.6$  [CA] the log-normal model more closely resembles the true knock intensity and therefore the knock intensity error at this point is lower. Note that fewer combustion cycles with relative spark angle  $DBL + 0.9$  [CA] and  $DBL + 1.6$  [CA] was recorded.



**Figure 5.4:** Knock intensity error for the Burr Type XII and Log-normal distribution estimates. Data was measured at operating condition 2000 rpm and 500 mg/stk. The  $Err(x_{0.95})$  can be seen in figure as knock intensity error at the 0.95 CDF value.

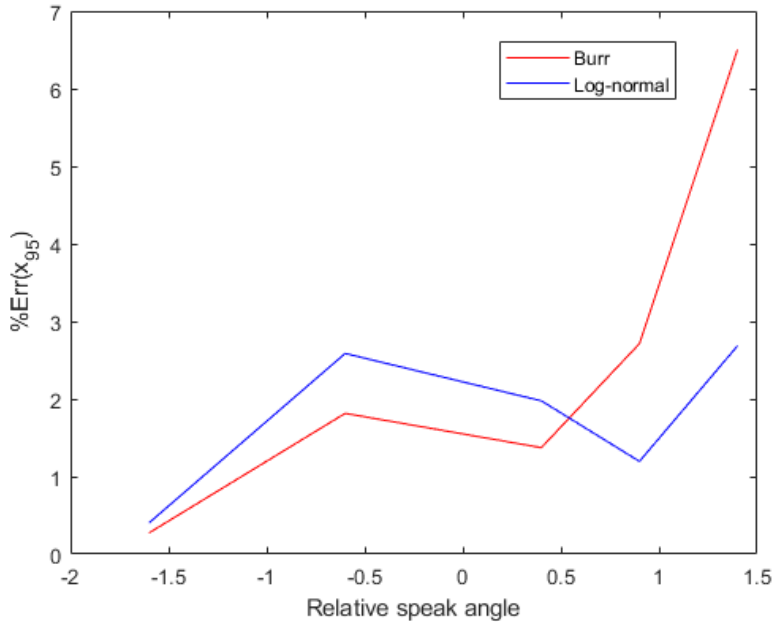


**Figure 5.5:** Percentage knock intensity error for the Burr Type XII and Log-normal distribution estimates at the 95:th percentile for different spark angles. The data collection was done at operating condition 2000rpm 500mg/stk.

## 5.2.2 Probability Error at Knock Event

The probability error at knock event calculated as equation (3.20) is shown for different ignition angles in figure 5.8. No knocking events occurred at  $DBL - 1.6 [CA]$  and the error was therefore defined as 0 in this case. The PDF estimates from the Burr Type XII model and log-normal distribution models can be seen in figure 5.6 and 5.7 respectively. By examining the PDF plots it is possible to distinguish the advantage of the Burr Type XII model. The log-normal model gives a satisfying result for the  $DBL - 1.6 [CA]$  data set but for more advanced spark angles it is not a good fit.

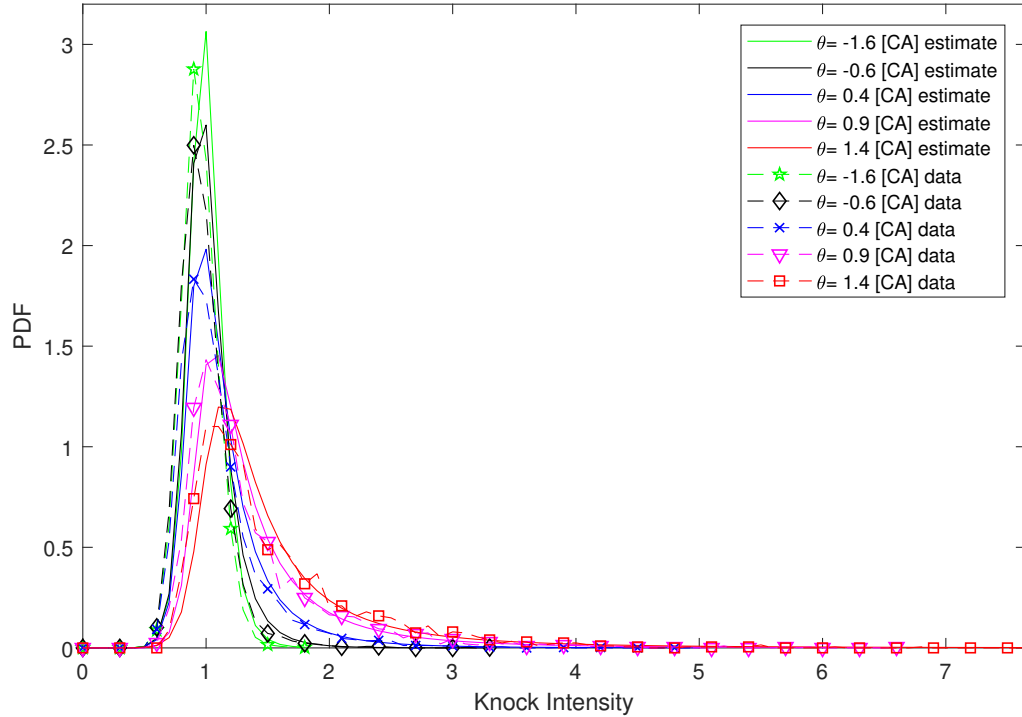


**Figure 5.6:** Estimated probability density function for different ignition angles for the gathered data shown in dashed lines along with the corresponding burr distribution estimations shown in solid lines. The plot visually shows how well the Burr Type XII PDF fits to the collected data.

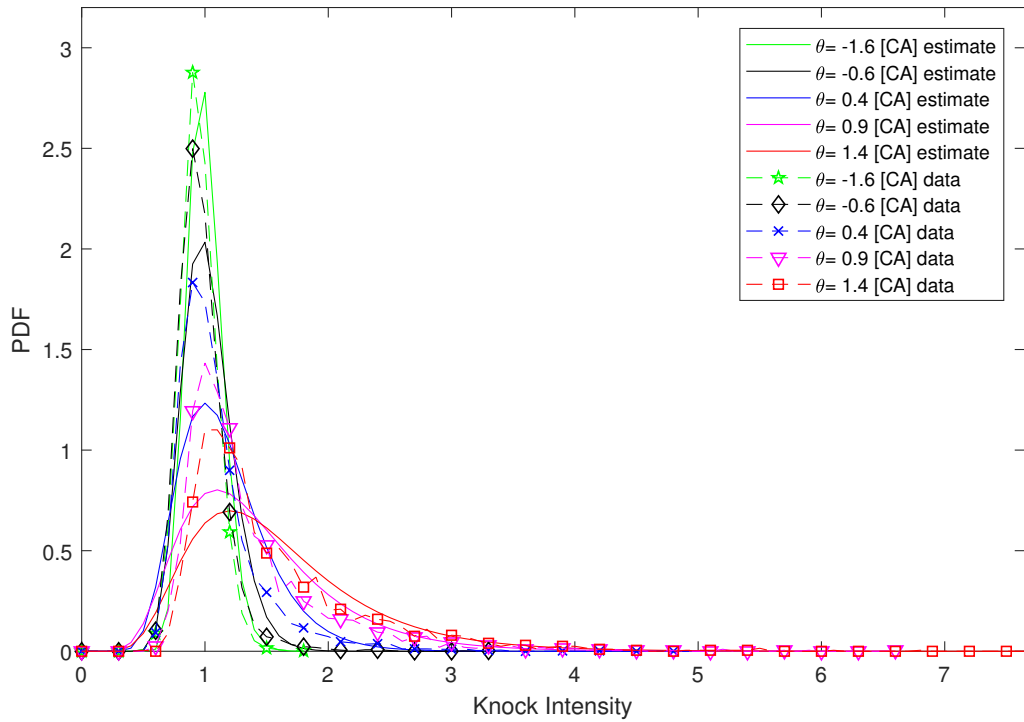


**Figure 5.7:** Estimated probability density function for different ignition angles for the gathered data shown in dashed lines along with the corresponding log-normal distribution estimations shown in solid lines. The plot visually shows how well the Log-normal PDF fits to the collected data.

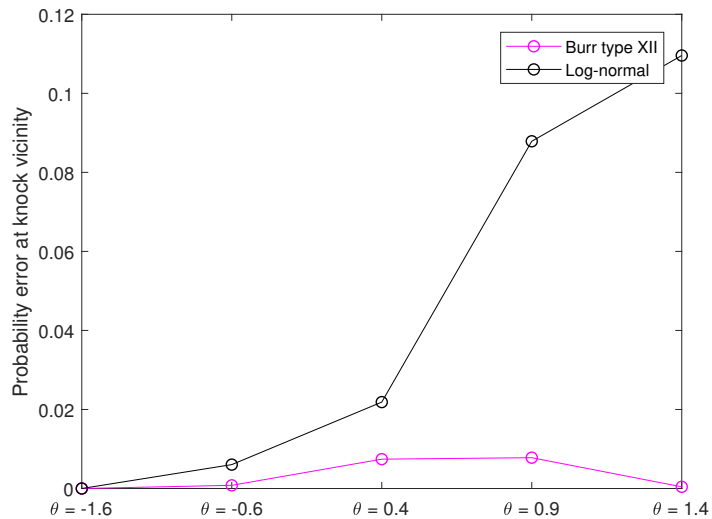


**Figure 5.8:** Probability error at knock threshold for burr and log-normal distribution estimation. The operating point when gathering data was 2000rpm 500mg/stk.

### 5.2.3 Kolmogorov-Smirnov Test Statistic

To validate the goodness of fit of the Burr Type XII and Log-normal distributions to knock intensity data, a kolmogorov-smirnov test was made. A significance level of  $\alpha = 0.05$  was used to calculate the critical values of the different data sets. The critical value increases for the more advanced spark angles as less data were gathered in these conditions. The test can be seen in Figure 5.9. According to the test it is possible to see that a log-normal distribution should be, at  $\alpha = 0.05$  level of significance, rejected for advanced ignition angles. The only ignition angle that should not be rejected is the most retarded ignition angle at  $-1.6$  CAs from DBL-timing. The Burr Type XII distribution should only be rejected for the most advanced ignition angle at  $+1.4$  CAs from DBL-timing whereas the other ignition angles falls inside the critical values and should not be rejected. Table 5.1 summarises the results of the different distribution model

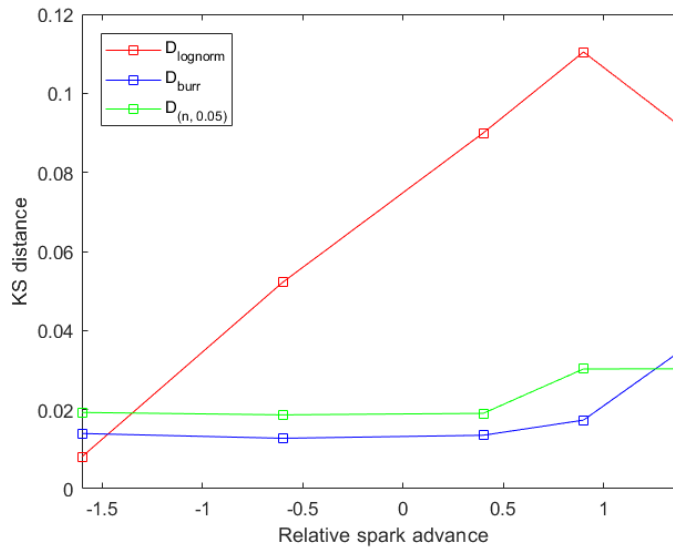


**Figure 5.9:** Kolmogorov-Smirnov test for Log-normal and Burr Type XII distribution. The green line is the critical value according to a significance level of  $\alpha = 0.05$ .

tests made in this thesis.

**Table 5.1:** Results for the log-normal and Burr Type XII distribution model validations. Here it can be seen that the Burr Type XII more closely describes the knocking intensities than the earlier suggested log-normal model.

Spark advance [CA]	Distribution model	KS	$Err(p_{0.01})$	$Err(x_{0.95})$	$\%Err(x_{0.95})$
DBL -1.6	Burr Type XII	0.0354	0.0672	0.0034	0.2732
	Log-normal	0.0910	0.0710	0.0050	0.4024
DBL -0.6	Burr Type XII	0.0173	0.0071	0.0246	1.8148
	Log-normal	0.1104	0.0056	0.0350	2.5867
DBL +0.4	Burr Type XII	0.0135	0.0010	0.0256	1.3728
	Log-normal	0.0900	0.0074	0.0368	1.9764
DBL +0.9	Byrr Type XII	0.0128	0.0016	0.0709	2.7134
	Log-normal	0.0522	0.0065	0.0312	1.9156
DBL +1.4	Burr Type XII	0.0140	0.0033	0.1974	6.5032
	Log-normal	0.0081	0.0015	0.0815	2.6853

### 5.3 Knock Control

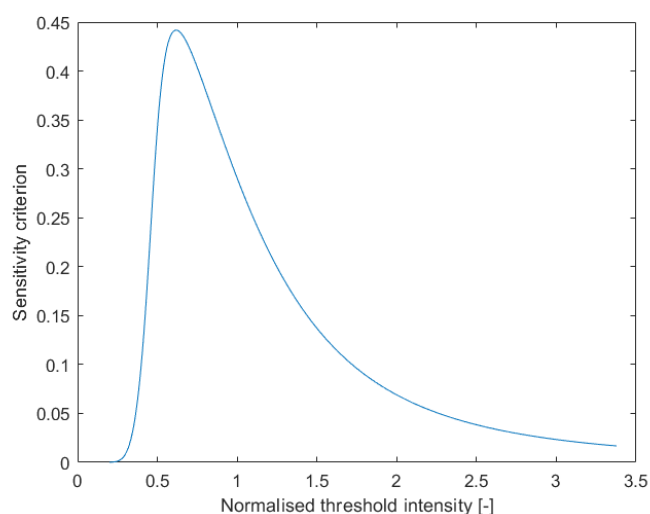
The knock controllers introduced in Chapter 2.3 were implemented and tuned in the simulation environment. The knock controllers were tuned for a desired knock probability of 1%. After tuning in the simulation environment they were implemented in a real four stroke turbo charged SI gasoline engine to validate the results. In this section, the final control parameters will be shown along with results both from the simulation environment and from the tests performed in the physical engine for the best performing knock controller of its type (Cumulative summation-based, Likelihood-based etc.). Except for the live estimation controller which were only implemented and tested in the simulation environment. Results from the other controllers can be found in appendix A. The operating condition both in the simulation environment and the real engine test were 2000 rpm, 500 mgair/stroke and lambda were set constant at  $\lambda = 1$ . The simulation results are shown as relative final ignition angle around the DBL. For real engine tests, the feedback signal was measured via INCA from the ECU. As earlier described, the crank angle is defined as positive after TDC. This requires the feedback signal to give a positive response when retarding the ignition timing and negative when advancing.

To clarify the plots of the knock controllers, relative ignition angle is shown for the results from the simulation environment and is defined as ignition angle relative to DBL-timing. This means that an ignition angle of 0 refers to DBL-timing. If the ignition angle is positive, then ignition angle is more advanced relative to DBL-timing and has a knock probability above 1%. In the results from real-engine tests, DBL-timing was unknown and therefore  $\Delta\theta_{ign}$  as defined in (2.1) is used. Its values will always positive since the knock controllers are tested in operating points where ignition angle is retarded from  $\theta_{ol}$  due to frequent knock events.

#### 5.3.1 Threshold Optimisation

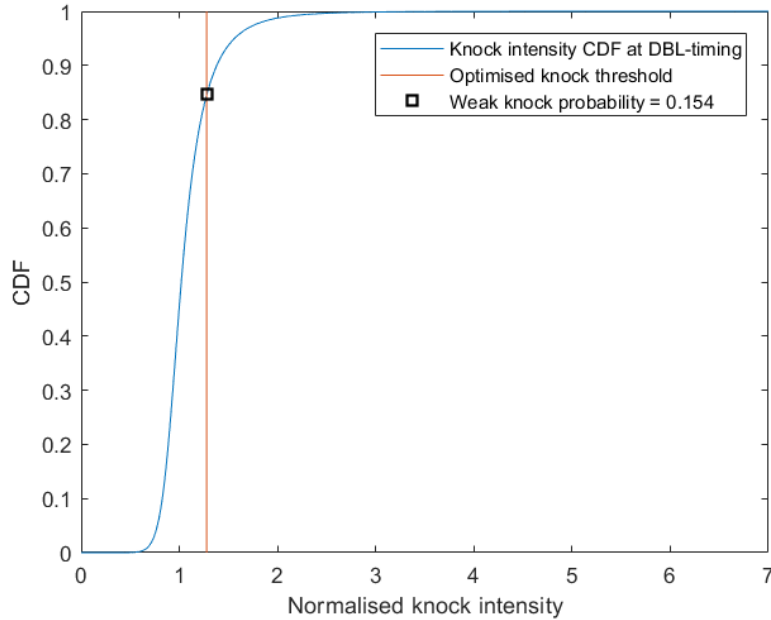
In section 3.4.4 knock threshold optimisation to increase the sensibility of the knock controllers by scaling the knock threshold were described. This was performed for the operating determined operating condition 2000 rpm 500mg/stk.

Figure 5.10 shows that the maximum sensitivity calculated using equation (3.29). In this operation condition the suggested knock intensity threshold scale is 0.6180 of the previously used knock threshold.



**Figure 5.10:** Sensitivity as a function of knock threshold performed on a single set of data. The maximum value occurs at a normalised threshold intensity value of 0.6180 which implies that the present threshold should be scaled with this factor.

In figure 5.11 the optimised knock intensity threshold is plotted against the knock intensity CDF from DBL timing conditions. The resulting weak knock rate is 15.4 % which means that the controllers tuned for weak knock rates targets a weak knock rate of 15.4 % to achieve a 1 % knock rate.



**Figure 5.11:** The figure illustrates the knock probability for a threshold that has been scaled with the derived factor that gives an optimal sensitivity.

### 5.3.2 Conventional Knock Control

A conventional knock controller was implemented and tuned in the simulation environment. Its retardation gain  $k_{ret}$  were set equal to  $1.6^\circ$  CA. Its advance gain could then be calculated to  $k_{adv} = 0.0162^\circ$  CA using (3.24) along with a target knock rate  $p = 1\%$ . In Figure 5.12 the saw-tooth behaviour of the conventional controller can be seen. The ignition angle is quite retarded relative to DBL-timing with peaks reaching well over DBL. The knock rate achieved from the controller converges towards the desired knock rate probability of 1%. To test the transient response, initial spark timing was set to  $\pm 2^\circ$  CA relative to DBL-timing. The transient responses from the conventional controller can be seen in Figure 5.13. The conventional controller is both fast in retarding the spark timing when the initial spark is too high and also quickly advancing from a rather low initial spark angle. This controller is commonly used in the industry today and will be used as a reference point to evaluate other controllers.

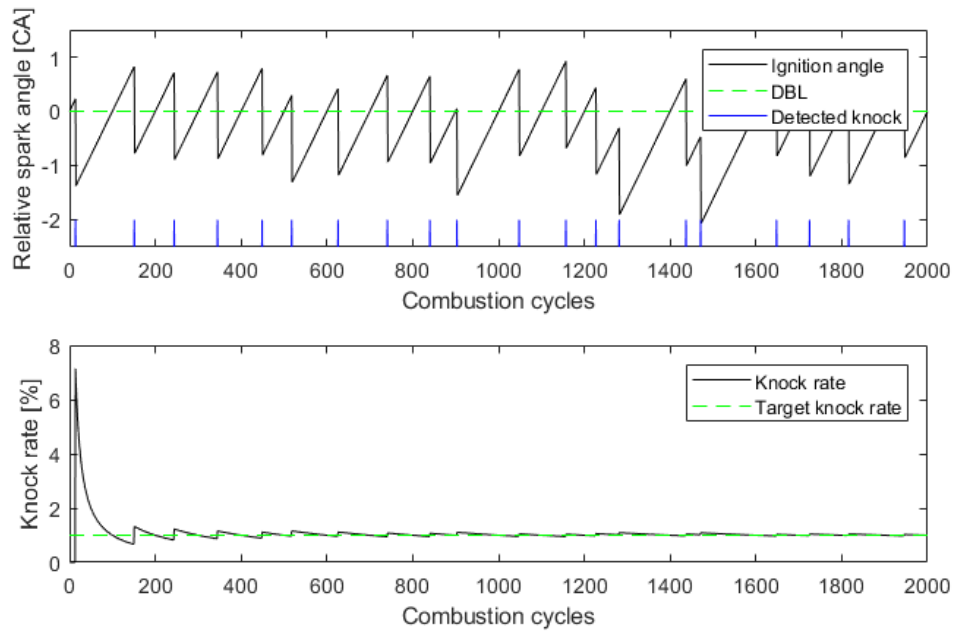


**Figure 5.12:** Simulation of the conventional controller ignition timing output in the simulation environment along with its achieved knock probability.

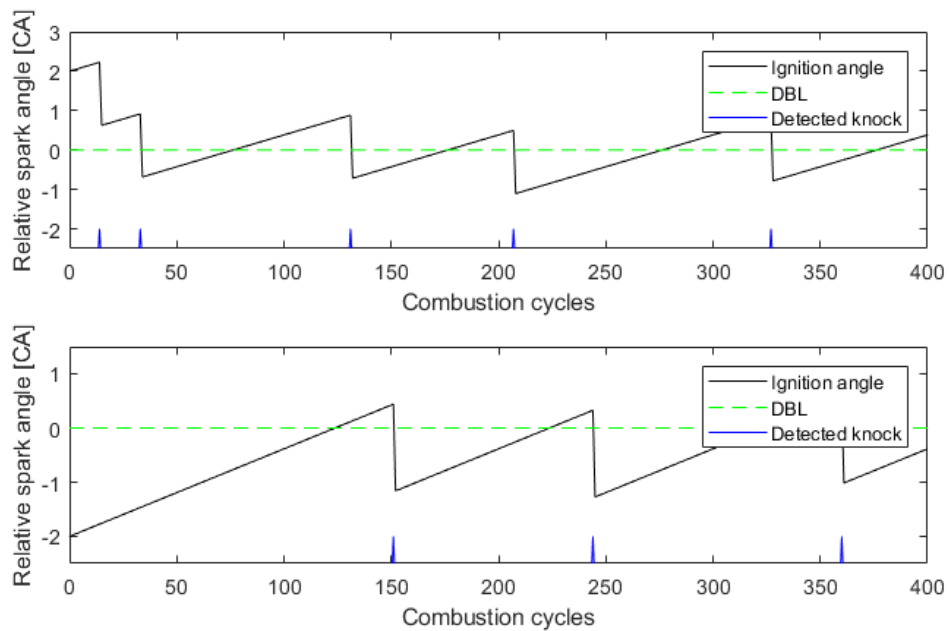


**Figure 5.13:** Transient responses for the conventional controller with initial spark angles of  $\pm 2^\circ$  CAs from DBL-timing.

### 5.3.3 Cumulative Summation Knock Control with Optimised Threshold and Likelihood-scaled Controller Gains

The cumulative summation knock controller described in section 3.4.2 was implemented in the simulation environment. Its threshold was optimised by scaling the knock threshold by a factor of 0.618 and its desired probability that determines the slope of parameter  $EK$  were set to  $p_{des} = 0.154$  as described in Section 5.3.1. The controller gains were set to  $k_{adv} = 0.33(1 - Ln)$  and  $k_{ret} = 0.45(1 - Ln)$  where  $Ln$  is the likelihood function described in section 3.4.3. The upper and lower boundaries determining when a spark adjustment should be done were set to  $u_{thr} = 1.5$  and  $l_{thr} = -1.5$  from the expected knock variable  $EK$ .

In Figure 5.14 steady-state condition for the controller can be seen. As a result from the optimised threshold, a more active controller is seen. The controller finds DBL quite well both in knock rate and spark angle. The knock rate oscillates around the desired 1% knock rate and ended after 2000 combustion cycles at around 1.15%. Transient response for the controller can

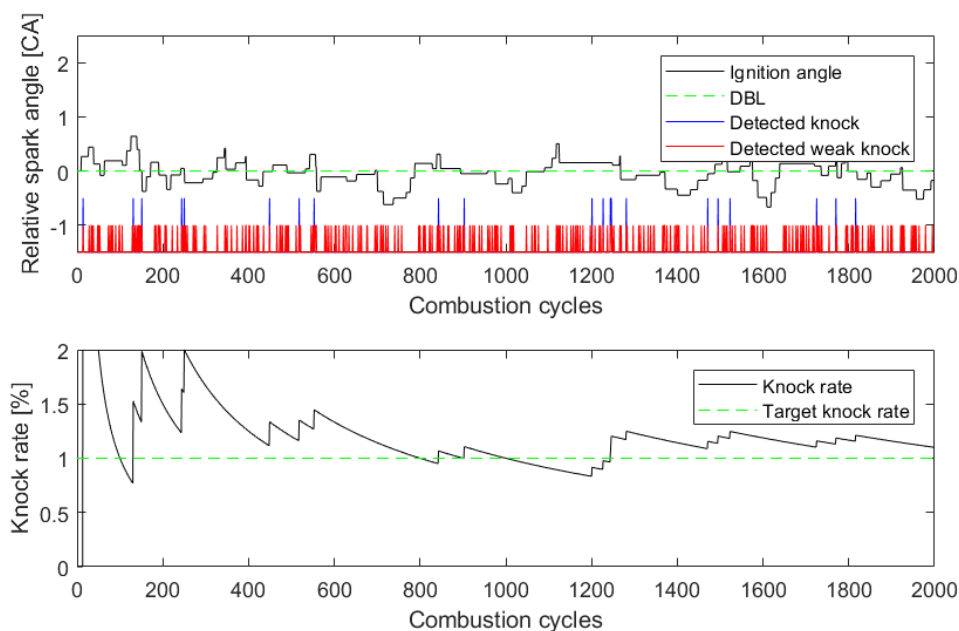


**Figure 5.14:** Spark angle and knock rate for threshold optimised cumulative summation knock controller with likelihood-scaled gains from simulation.

be seen in Figure 5.15 were spark angle were initially set  $+2^\circ$  and  $-2^\circ$  CA from DBL. In both cases, the controller acts quickly and sets the spark angle around DBL-timing. For the initially retarded spark angle it reached DBL-timing 126 combustion cycles which is around the same for the conventional controller (124 cycles for conventional.). For the initially advanced spark angle, it takes two detected knocks to reach DBL-timing and 50 combustion cycles.

Test results from the real engine steady-state tests are shown in Figure B.1 in Appendix B. Similar results were held in the physical engine as for the simulation results seen in Figure 5.14 and a knock-rate of 1.17% were reached after around 2000 combustion cycles which corresponds well to the simulation tests. In Figure B.2 in Appendix B the transient response of the controller can be seen in real engine test. Instead of  $\pm 2^\circ$  CA a transient of  $6^\circ$  CA was tested. for the overly retarded ignition angle the fast advancement can be seen. For the overly advanced ignition angle there is an initially quick response that declines with time. By examining the plot it is possible to see that no knocks occurs between cycle 210-415 but the ignition angle keeps reducing until it reaches its normal value again after around 450 combustion cycles.

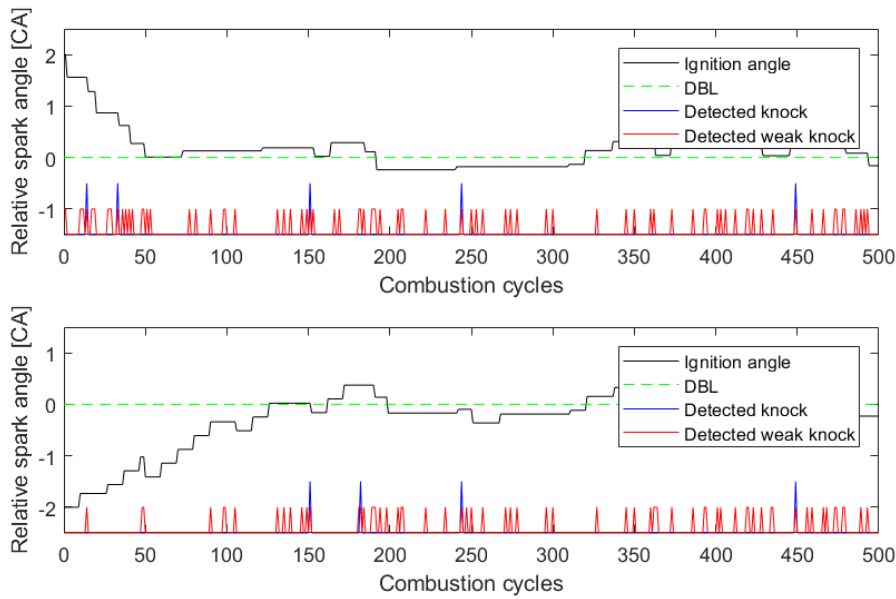


**Figure 5.15:** Transient responses with spark angle disturbances of  $\pm 2^\circ$  CA from DBL-timing for the threshold optimised cumulative summation knock controller with likelihood-scaled gains from simulation.

### 5.3.4 Conventional Control with Optimal Threshold

By performing a sensitivity analysis according to section 3.4.4 and calculating the optimal threshold and the corresponding knock probability it is possible to re-tune the conventional controller. Setting the retard gain to  $k_{ret} = 0.2$  the advance gain can be calculated using expression (3.24) and new knock rate. This results in  $k_{adv} = 0.1540 / (1 - 0.1540) \times 0.2 = 0.036^\circ$ . The controller performance when initialised at DBL ignition angle can be seen in figure 5.16.

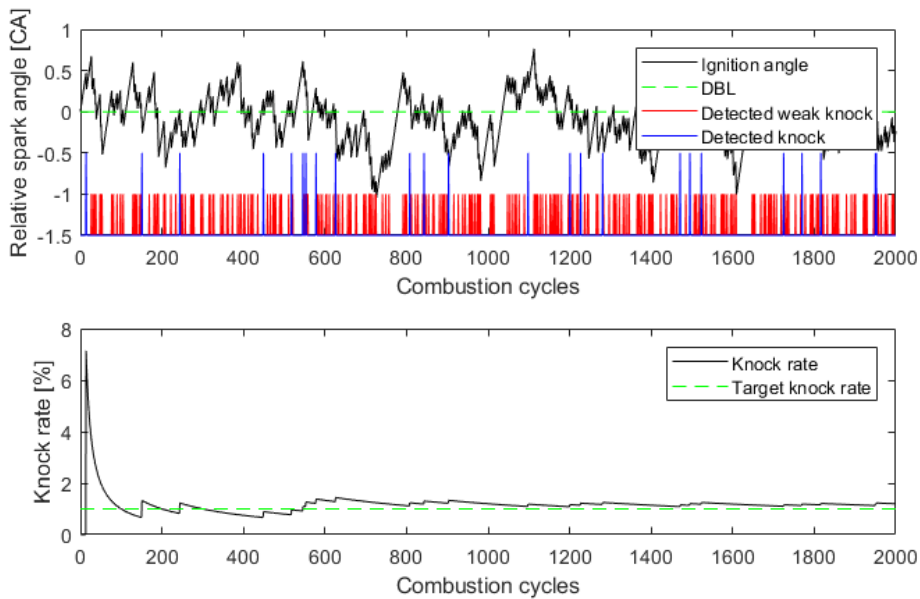


**Figure 5.16:** Spark angle and knock rate for the conventional controller with optimised threshold.

The resulting controller is very reactive due to the lowered threshold. However, since the spark adjustment gains are lowered when compared to the conventional controller, the spark angle is less disperse. The overall knocking probability settles at around 1 % as intended.

Figure 5.17 shows the transient response of the controller when initialised with  $\pm 2$  CA from DBL.

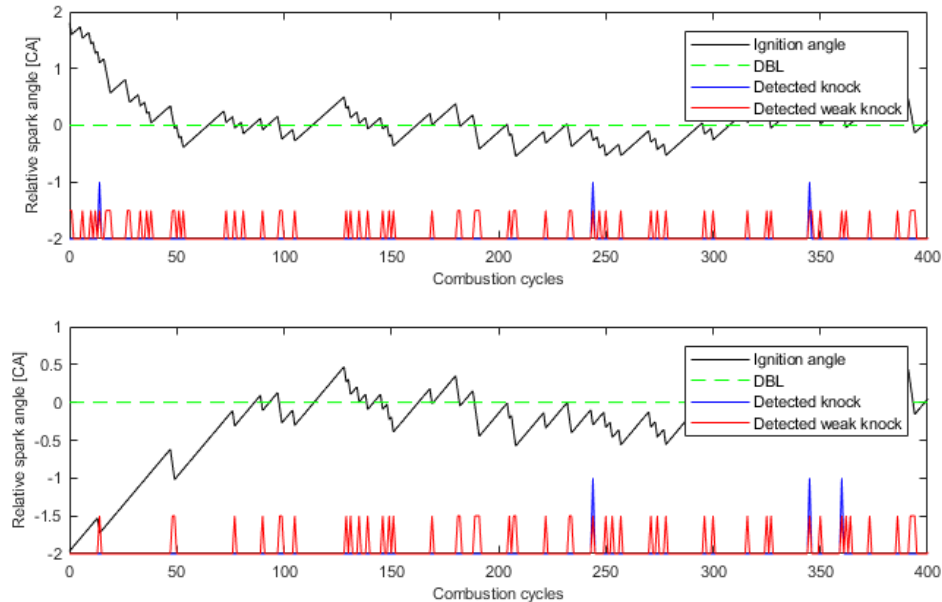


**Figure 5.17:** Spark angle transient response for the conventional controller with threshold optimisation from simulation. Initial spark was set  $\pm 2^\circ$  CA from DBL-timing.

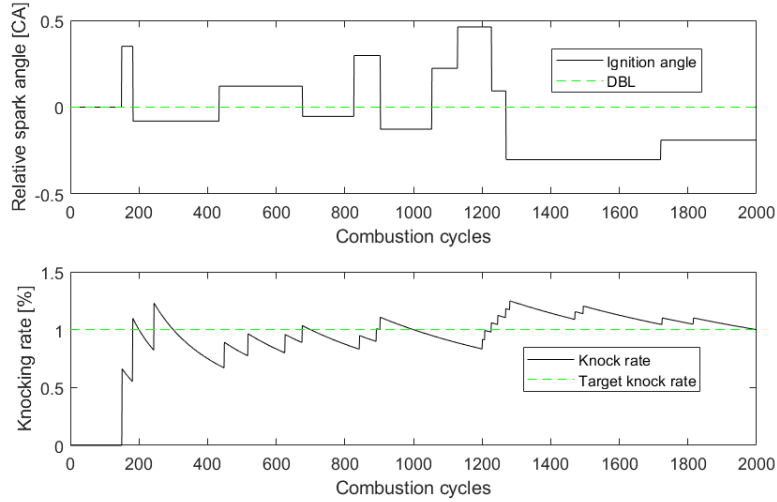
The controller manages to retard the ignition angle when starting in a overly advanced state in approximately 50 cycles, only experiencing one knock. The spark advance from the overly retarded spark angle to DBL occurs after some 100 cycles. These results are comparable if not even better in terms of transient response when compared to the conventional controller. This in combination with the reduced spark dispersion promising results.

Figure B.3 in Appendix B shows the resulting ignition timing feedback from the controller along with the knock probability from real engine tests. A final knock rate of 1.67% were held from the experiment which is relatively high. The solid green line is the feedback part of the controller described in equation (2.1) measured from the vehicle ECU.

The knocking probability during this data collection does not reach the target level of 1 %, implying that the controller acts too aggressively. The transient response from real engine tests is left out for this controller due to incorrect feedback signal and corresponding final ignition angle. This is discussed further in chapter 6.

### 5.3.5 Likelihood knock control with fast-forward algorithm

A likelihood-ratio algorithm based knock controller was implemented according to section 3.4.3 followed by tuning of its control parameters. The likelihood-ratio threshold was set to  $Ln_{thr} = 0.4$ , the retard gain was set to  $k_{ret} = 0.6$  and the advance gain was set to  $k_{adv} = 0.3$ . The feed-forward algorithm was used with parameter  $k_0 = [0, 20, 40, 60]$ . Figure 5.18 shows the controller behaviour when initialised at DBL-angle. The controller results in a overall satisfying knocking



**Figure 5.18:** Spark angle and knock rate results for the likelihood-controller with fast-forward algorithm from simulation.

probability of 1 % while keeping the spark dispersion low and close to DBL. The transient response for the controller can be seen in figure 5.19. The initial spark angle was adjusted +2 and -2 from DBL. The knock detection signal is also shown in the figure to highlight the potential danger of a transient with this statistically based controller configuration.

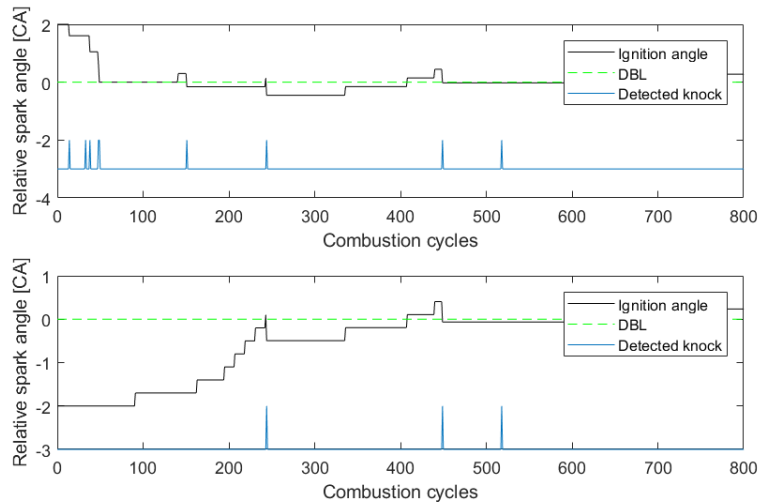


**Figure 5.19:** Likelihood-ratio controller with fast-forward algorithm result with initial spark angle offset. The spark angle was initiated at  $\pm 2^\circ$  CA from DBL-timing.

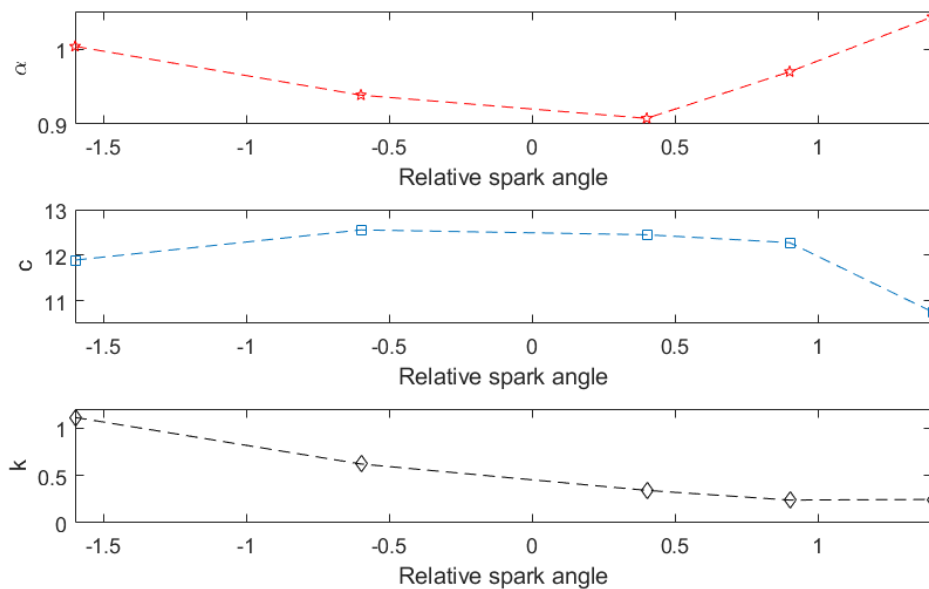
The controller reduces the spark angle to DBL in approximately 50 combustion cycles, experiencing 4 knocks. The results are somewhat satisfactory. Due to the nature in how the ignition timing is retarded, there appears a cluster of knocking combustions. Clusters of knocking cycles are highly unwanted since repeated knocking cycles can harm the engine. However, the ignition timing is restored to DBL in an acceptable amount of cycles. The controller advances from DBL  $-2^\circ$  and reaches DBL in approximately 250 cycles. Compared to the conventional controller this is a slower advance, however, the spark is kept at a close vicinity of the DBL ignition timing.

Figure B.4 In Appendix B shows real engine tests for the controller. In the first 1000 cycles the controller makes no action and keeps the ignition angle stable since the number of knocking cycles are in close correspondence to the target rate of 1 % but undershoots a little. This is an interesting result and highly different to the conventional controller. The overall knock rate in this data set reveals that in this case the controller could be a bit more aggressively tuned.

Figure B.5 in Appendix B, transient responses from real engine tests are shown. The transient response is similar to the simulation result. The offset for this test was set to  $\pm 3^\circ$  to give the controller a challenge. The controller responds well to an ignition angle disturbance that suddenly advances the ignition angle 3 degrees. The controller advances the ignition angle according to the fast forward implementation and works as intended.

### 5.3.6 Live estimation knock control

From the spark sweep data, the parameters  $\alpha$ ,  $c$  and  $k$  from the burr distribution were calculated. a plot of the parameters of the operating point 2000rpm, 500mgair/stroke and  $\lambda = 1$  can be seen in Figure 5.20. Since both  $\alpha$  and  $c$  has two solutions for most ignition angles, only  $k$  is chosen as the reference signal to determine if an advance or retard should be executed.



**Figure 5.20:** Estimated  $\alpha$ ,  $c$  and  $k$  variable from data gathered from a spark sweep experiment at 2000rpm, 500mgair/stroke and air-fuel ratio such that  $\lambda = 1$  were achieved. Relative spark angle is shown were 0 is DBL-timing and positive values refer to an advancement from DBL-timing.

Knock factors were calculated from CDFs for different sample sizes in the simulation environment and the variance of these knock factors can be seen in Appendix A.7. The variance

decreases significantly for increasing sample sizes to around size 45 and is held quite constant after. a sample size of 45 knock intensity samples were considered too long though and thus, a sample size of 25 samples were instead selected in the controller.

The  $k$  parameter value for DBL-timing were calculated to  $k_{DBL} = 0.45$  and a deviation of  $k = k_{DBL} + 0.24$  were set to make a spark advance whilst  $k = k_{DBL} - 0.13$  will trigger a retard action. These values were arbitrary chosen based on the decreasing difference in the  $k$  parameter for higher spark angles as seen in Figure 5.20. Fixed spark angle steps were chosen to  $k_{adv} = 0.15$  and  $k_{ret} = -0.4$ . Since fixed advance gains were used the controller transient responses are worsened. To speed up the retard response, a safety algorithm is included that if 30% of the last 10 cycles were knock events, spark should be retarded by 1 CA. Similarly, a fast-forward algorithm were introduced that counted the last spark advances such that if the controllers last control action was an advance action, it will scale up the advance gain by a factor  $adv_{scale}(adv_{count})$ . This scaling factor keeps increasing if more advance actions are present in a row. based on this, the fixed advance gain were scaled by the factors:  $adv_{scale} = [1, 1.25, 1.75, 2.5]$ .

A simulation of the live estimation controller for 2000 combustion cycles can be seen in Figure 5.21. The controller is able to find DBL-timing relatively well and deviates less than 1 CA as most.

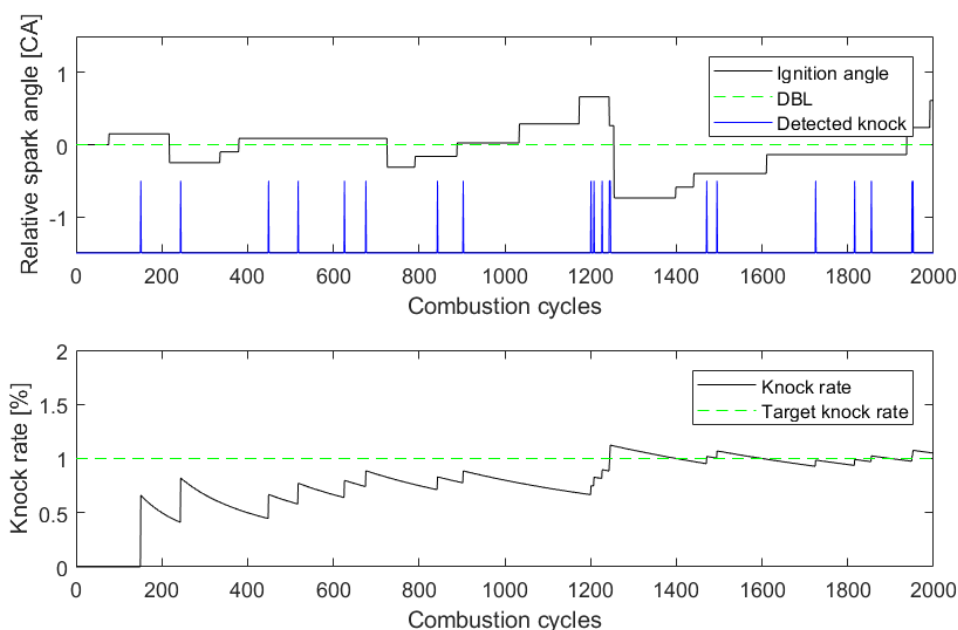


**Figure 5.21:** Steady-state simulation of the live-estimation controller with an initiated spark angle at DBL-timing is shown. Achieved spark angle and knock rate is shown.

Transient responses for the controller is visible in Figure ???. The controller acts relatively slow on the ramp up case were it reaches DBL-timing after around 340 cycles. For initially advanced spark angles it reaches DBL-timing in about 50 cycles were 7 knocks were recorded.

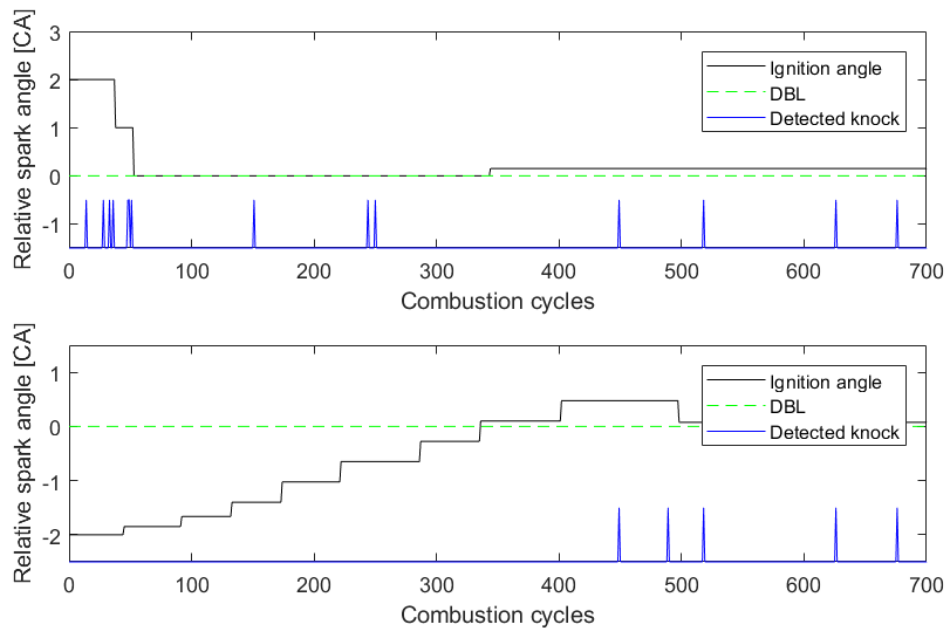


**Figure 5.22:** Transient response simulation for the live-estimation controller with an initiated spark angle disturbance of  $\pm 2^\circ$  CA from DBL-timing. Spark angle from the two different ignition angle disturbances are shown.

## 5.4 Side-by-side Comparison of Knock Controllers at Steady-state Operation

To compare the different knock controllers, all of them were simulated against the same seed of uniformly generated random numbers in the simulation environment. The controllers will be referred to their abbreviation which can be seen in parenthesis under the "Knock controller" column in Table 5.2 and Table 5.3.

Steady-state simulation was performed where all knock controllers start at DBL ignition timing for 50 000 combustion cycles. The data is presented in table 5.2. As seen in the table, the controller closest to DBL-timing is the LE knock controller which mean ignition angle is just 0.053 CA from DBL-timing. It is closely followed by the Conv\_ThrOpt which ended up with a mean ignition angle at 0.058 CA from DBL-timing. Both the LE and Conv\_ThrOpt controllers had slightly high knock probabilities with a knock rate of 1,20% and 1,28% respectively. All of the knock controllers achieved a lower max knock intensity and significantly reduced knock variance compared to the conventional strategy. The mean ignition efficiency was calculated to give perspective to how a mean relative ignition relates to efficiency. It was calculated using a commonly used efficiency table that gives an efficiency for a certain ignition timing. The characteristics of the ignition efficiency compared to ignition timing resembles the function for torque output which can be seen in Figure 2.3. In the ignition efficiency table, DBL-timing was set  $-10^\circ$  CA from MBT-timing. 100 % efficiency is, in this case, MBT ignition timing.

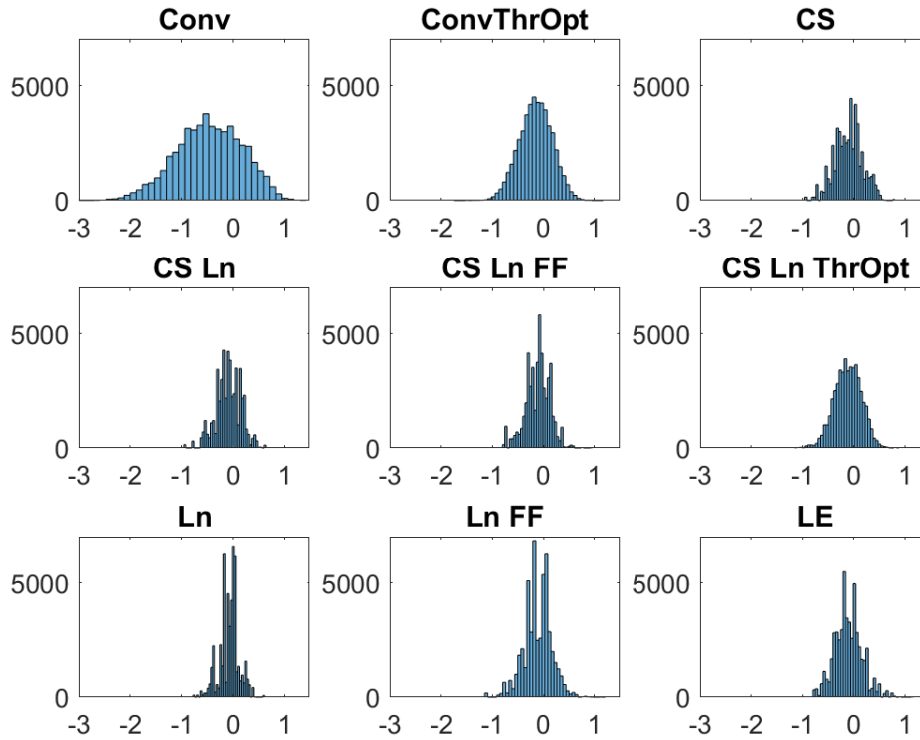
**Table 5.2:** Simulation results from all implemented knock controllers.

Knock controller	Mean relative ignition angle [CA]	Ignition angle variance [CA]	Knock rate [%]	Mean ignition efficiency [%]	Max knock intensity [-]
Conventional (Conv)	-0,467 (-)	0,4174	1,00	90,91 (-)	9,73
Cumulative summation (CS)	-0,104 (+0,363)	0,0785	1,05	91,44 (+0,53)	7,33
Cumulative summation with likelihood-scaled controller gains (CS_Ln)	-0,093 (+0,374)	0,0521	0,97	91,46 (+0,55)	6,57
Cumulative summation with likelihood-scaled controller gains and fast-forward algorithm (CS_Ln_FF)	-0,109 (+0,358)	0,056	0,97	91,43 (0,52)	5,84
Cumulative summation with likelihood-scaled controller gains and optimised threshold (CS_Ln_ThrOpt)	-0,089 (+0,378)	0,0749	1,06	91,46 (+0,55)	6,27
Likelihood (Ln)	-0,163 (+0,304)	0,0541	0,82	91,36 (0,45)	6,17
Likelihood with fast-forward algorithm (Ln_FF)	-0,121 (+0,346)	0,0657	0,96	91,42 (+0,51)	8,19
Conventional with optimised threshold (CS_ThrOpt)	-0,058 (+0,409)	0,1020	1,28	91,50 (+0,59)	8,61
Live estimation (LE)	-0,053 (+0,414)	0,0830	1,20	91,50 (+0,59)	8,61

Due to the variability in knock probability, the controllers were slightly re-tuned to have matching knock probabilities. The same simulation seed as for the simulation in Table 5.1 was reproduced. The simulation results along with the changed parameters can be seen in Table 5.3. Note that the transient responses might have been slightly changed after this re-tuning. The new results shows that Conv\_ThrOpt and LE knock controllers were advanced in previous simulation due to their high knock rate. As the likelihood controller was re-tuned, its spark angle advanced significantly to -0,073 CA from DBL-timing. The resulting ignition angle relative to DBL can be seen in Figure 5.23. The statistically based controllers as well as the threshold optimised conventional controller manages to keep the ignition timing closer to DBL and experiences less dispersion compared to the conventional controller.

**Table 5.3:** Steady-state simulation results of 50 000 combustion cycles of the re-tuned knock controllers to achieve a knock probability of 1%.

Knock controller	Changed control parameters	Mean relative ignition angle [CA]	Ignition angle variance [CA]	Knock rate [%]	Mean ignition efficiency [%]	Max knock intensity [-]
Conventional (Conv)	-	-0,467 (-)	0,417	1,00	90,91 (-)	9,73
Cumulative summation (CS)	$k_{ret} = -0,51$ $k_{adv} = 0,43$	-0,104 (+0.363)	0,072	1,01	91,44 (+0.53)	7,81
Cumulative summation with likelihood-scaled controller gains (CS_Ln)	$k_{ret} = -0,64$ $k_{adv} = 0,56$	-0,090 (+0.377)	0,057	1,01	91,46 (+0.55)	7,51
Cumulative summation with likelihood-scaled controller gains and fast-forward algorithm (CS_Ln_FF)	$k_{ret} = -0,64$ $k_{adv} = 0,56$	-0,108 (+0.359)	0,055	1,01	91,44 (+0.53)	8,18
Cumulative summation with likelihood-scaled controller gains and optimised threshold (CS_Ln_ThrOpt)	$k_{ret} = -0,46$ $k_{adv} = 0,31$	-0,118 (+0.349)	0,069	1,01	91,42 (+0.51)	5,81
Likelihood (Ln)	$k_{ret} = -0,41$ $k_{adv} = 0,39$	-0,073 (+0.394)	0,042	0,99	91,48 (+0.57)	6,97
Likelihood with fast-forward algorithm (Ln_FF)	$k_{ret} = -0,6$ $k_{adv} = 0,33$	-0,108 (+0.359)	0,073	1,01	91,44 (+0.53)	8,18
Conventional with optimised threshold (Conv_ThrOpt)	$k_{ret} = -0,2$ $k_{adv} = 0,0326$	-0,150 (+0.317)	0,104	1,00	91,38 (+0.47)	6,44
Live estimation (LE)	$k_{ret} = -0,38$ $k_{adv} = 0,15$ Retard if $k < k_{DBL} - 0,18$ Advance if $k > k_{DBL} + 0,6$	-0,108 (+0.317)	0,071	1,01	91,38 (+0.47)	6,44

**Figure 5.23:** Histogram showing the relative spark angle for the different controllers. The results were obtained from the simulation environment for 50000 combustion cycles.

## 5.5 Background noise evaluation

The two different strategies to estimate background noise described in Section 3.1.1 and 3.1.2 were first implemented in the simulation environment to be tested and calibrated. They were then implemented in the engine for tests in the real environment. The step length in the low-pass noise estimator was calibrated to  $noise_{adv} = 0.01$ . In the low-pass noise estimator, 30 knock power samples were considered to produce a good balance between acceptable estimation and response in transients. The noise estimators were tested in the simulation environment both in

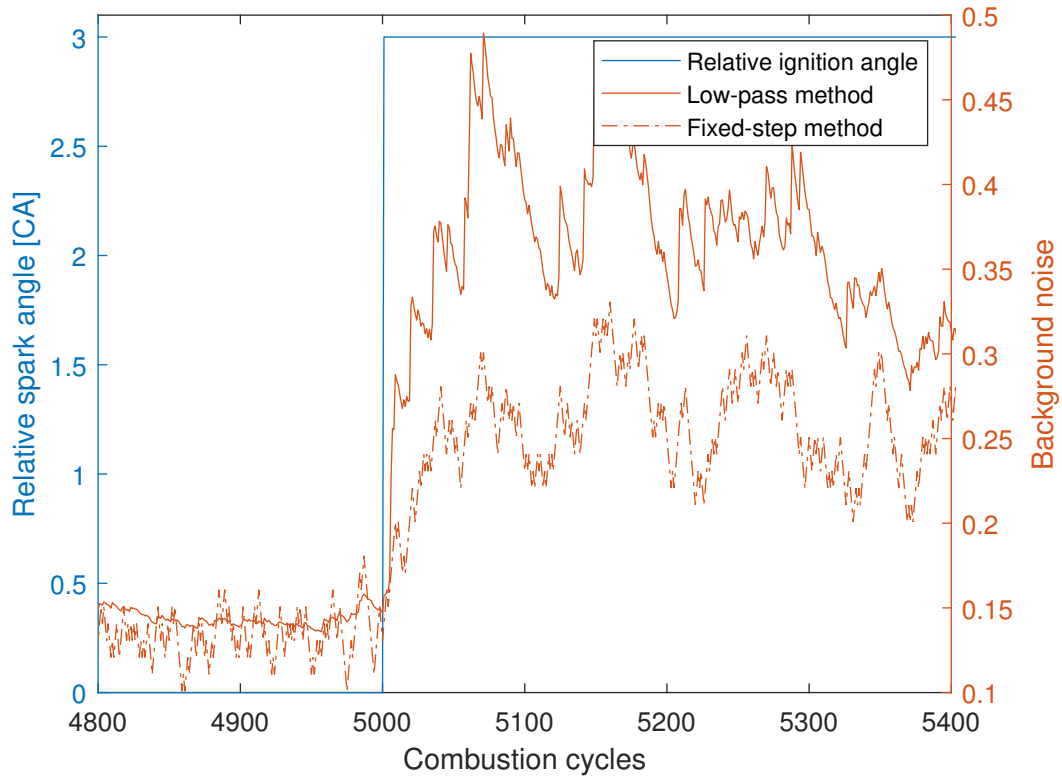


**Figure 5.24:** Simulation of the fixed-step and low-pass filter noise estimators with a transient response of  $+3^{\circ}\text{CA}$  at cycle number 5000.

steady-state and transient response by a step in ignition angle. Figure 5.24 shows the methods response as ignition angle increases from DBL-timing to  $+3$  CA from DBL-timing. As the step is initiated at combustion cycle number 5000, a lag in the low-pass method is visible before it starts to increase. The fixed-step method does not lag before it increases and ramps up relatively fast before it starts to vacillate between  $0.2 - 0.3$  which is a relatively large area.

In Figure 5.25 steady-state results from the same simulation as above can be seen. At DBL-timing (4800-4900 cycles), both noise estimations hold relatively even noise levels where the fixed-step method differs more than the recursive. Clear difference between these noise estimation techniques is seen at DBL+3-timing (5000-5150 cycles). Here the low-pass method is constantly higher than fixed step method and high noise peaks occur due to the high knock power signal caused by the highly frequent knock events and their increased value in this ignition angle. The knock classification between these two methods will therefore differ a lot in this operating condition and will significantly affect the knock controllers since it affects the knock intensity signal according to (3.1).

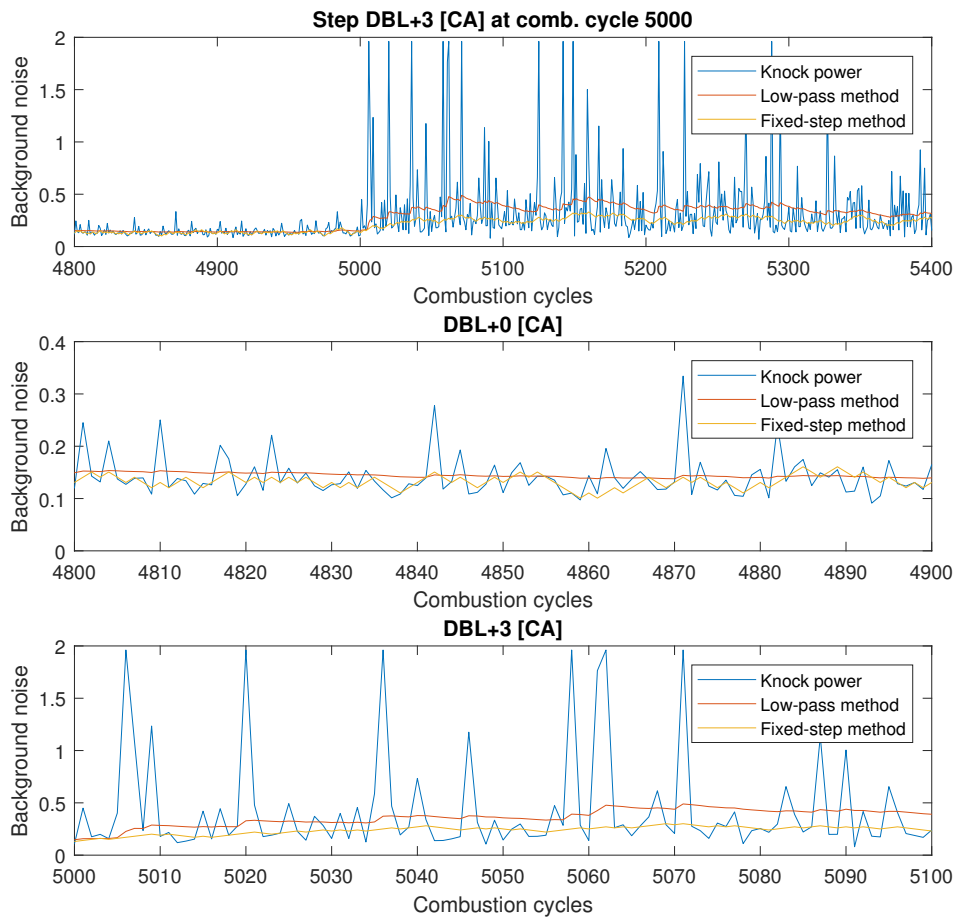


**Figure 5.25:** Illustration of how the background noise level changes with knock power. For DBL timing the methods give an equal noise level. Even though the fixed step method is a more reactive. However, when the ignition angle is advanced the low-pass method is consistently higher, thus requiring a higher knock power for the normalised signal to exceed the threshold level.

# Chapter 6

## Discussion

---

**Distribution estimation** As earlier described, a simulation environment that describes the combustion process is of great value when developing, analysing and evaluating different knock control algorithms. The Burr Type XII distribution model was shown to be a great estimation of knock intensity. Figure 5.9 shows that the Burr Type XII distribution model only should be rejected for the most advanced spark angles. This is an improvement when compared to the log-normal distribution model. However, since data gathering was executed in a test vehicle that had to be handled with care, less data was collected for the more advanced ignition angles where more frequent audible knock events occur. This led to sparsely distributed data in the higher knock intensity values, see Figure 4.5. If a more extensive collection of data was obtained at these ignition angles, the estimated Burr Type XII distribution model could perhaps give a closer fit and not be rejected. The knock intensity error in figure 5.5 shows that the log-normal model gives a better result than the Burr Type XII model for advanced spark angles. It is worth noting that the knock intensity is overall described more closely by the Burr Type XII model.

**Knock control strategies:** The conventional controller with optimal threshold would not require a reconstruction of the current feedback system, but quite simply a scaling of the threshold map and re-tuning of the gain parameter maps which perhaps makes it even more desirable. Since the statistically based and optimal threshold controllers have a reduced spark dispersion and a mean that is closer to DBL the knock intensity distribution will contain less harmful and NVH-inducing and knocking events. Thus, the knocking probability of 1 % is of lesser importance. Since if both the conventional and conventional controller with optimal threshold aims at a knock rate of 1 % the conventional will obtain unnecessarily advanced ignition timings and experiencing overall knocking events with higher intensities, even though the rate is still 1 %.

Maximum knock intensity for the statistical knock controllers is reduced compared to the conventional approach as a result of not advancing too far from DBL-timing. As the aim of a conventional knock controller is to control the ignition timing such that a knock rate of 1% is attained, this knock rate could be increased for the stochastic knock controllers without experiencing higher knock intensities than the conventional approach. In Table 5.2, both LE and Conv\_Thropt had significantly higher knock rates than conventional controller (1.20% and 1.28% respectively) without the increase in maximum knock intensity. Therefore an interesting parameter to be aimed at in addition to knock rate, would be to limit knock controllers to a maximum knock intensity. This would lead to a higher knock rate permission for operating points of low load which decreases as load increases as higher knock intensities are prone to appear in those conditions.

The real engine tests of the controllers were just performed for around 2000 combustion cycles. As the stochastic behaviour of knock is apparent, it should be noted that the knock rate can

differ quite a lot from experiment to experiment for tests of just 2000 combustion cycles with the same controller tuning. To be sure that the controllers from the real engine tests achieve a knock rate of 1%, extensive testing is required. This could not be done in this thesis due to limited time in the test rig.

**Knock detection:** A closed loop knock control system is highly dependent on a well performing knock detection system. When calculating the background noise for controllers that allow knocking combustion to occur without spark adjustment there lies a risk that the background noise level increases to unnecessarily high values and thus, decreases the chance to detect a knock event. The fixed-step background noise estimation is a way of dealing with this problem and was shown to work as intended. The low-pass filter estimation of the background noise level could be improved. The implemented structure based noise level on all knock intensities. if instead knock intensities that were classified as a knock combustion were not considered in the calculations, its performance would probably be improved. Another add-on that might prevent the low-pass filter from peaking at high knock intensities would be to maximise the allowed input from a single knock intensity value.

# Chapter 7

## Conclusions and Future Work

---

### 7.1 Conclusions

The cyclical dependencies of knock intensity were investigated using autocorrelation analysis with the results that knock intensity is a cyclically uncorrelated process and can therefore be described by its probability density function. The Burr Type XII distribution model was found to fit the knock intensity in operating condition 2000rpm 500 mgair/stk. with significance level  $\alpha = 0.05$  for all tested ignition timings except for the most advanced. To put the Burr model into perspective it was compared with the widely used Log-normal distribution model and was proven to give a better fit, see section 5.2 and table 5.1.

A knock intensity driven simulation model based on the Burr Type XII distribution was implemented in MATLAB & simulink with good results. The simulation model was used to examine knock intensity and to implement, tune and evaluate different kinds of knock feedback controllers. The controllers that showed most interesting result in simulation were implemented and evaluated in a Volvo four-stroke engine. Real engine tests showed similar results to the simulation. The live estimation controller showed great prowess in simulation. In real engine the threshold optimised conventional and cumulative summation as well as the fast forward likelihood controller gave interesting results and should be considered as challenging contenders to the widely used conventional controller. A number of different methods and types of knock feedback controllers were implemented and tested, both in the simulation environment and in a physical four cylinder Volvo engine. A common problem with most stochastic controllers is its race between fast transient response and ability to keep spark timing at DBL-timing. Table 5.2 shows results from steady-state operating in simulation. All implemented controllers were able to keep a more advanced spark angle compared to the conventional strategy whilst still lowering the maximum knock intensity peak in steady-state operation. The variance of ignition timing from the implemented controllers were significantly reduced compared to the conventional controller. The threshold optimised controllers aiming for a weak knock rate were able to behold the same ramp-up transient response as the conventional controller. Spark angle can therefore be advanced whilst still behold the same aggressiveness towards DBL-timing if an unnecessarily retarded spark timing is apparent.

The statistically based knock controllers which aimed at a knock rate of 1% performed better than the conventional controller in steady state operation, with a reduction in spark dispersion and improved mean spark advance. They had a slight reduction in transient response even for the fast forward improvement add-on. The sensitivity analysis threshold optimised controllers proved to give good results in both steady state and transient operation. Improved mean spark advance, lessened spark dispersion and a reduction in maximum knock intensity in combination with comparable result in transient response makes these two controllers very promising.

## 7.2 Future work

Further evaluation of the burr type XII distribution model by gathering longer data sets in the more advanced ignition angles is of interest. The data sets used in this thesis in the most advanced ignition angles had limited data due to the occurrence of frequently audible knocks. To minimise the risk of engine failure, shorter data sets were therefore used.

The simulation environment that was created could only generate knock intensities for one operating condition. If knock intensity data from spark sweep experiments were obtained in a wide range of operating conditions, distribution parameters could be estimated to form a more complete simulation environment able to simulate drive cycles.

With the Burr Type XII shown estimate knock intensities with great precision, questions arise whether the inverse could be done in a control perspective. The live estimation controller is a first step to creating such a controller. A controller that uses information about previous combustion cycles to estimate the current knock intensity distribution and compares it to a desired distribution and uses this information to make spark adjustments could prove to perform great.

A improvement of the low-pass filtered background noise calculation could be done by excluding knock intensities that exceeded the knock threshold in the calculation.

# Bibliography

---

- [1] J. Heywood, *Internal Combustion Engine Fundamentals*. McGraw-Hill Professional, 1988.
- [2] L. Eriksson and L. Nielsen, *Modeling and Control of Engines and Drivelines*. John Wiley & Sons ltd., 2015.
- [3] N. Cavina and A. Businaro, “Knock control based on engine acoustic emissions: Calibration and implementation in an engine control unit,” *SAE International*, 2017.
- [4] F. Millo and C. V. Ferraro, “Knock in s.i. engines: A comparison between different techniques for detection and control,” *SAE International*, 1998.
- [5] S. M. Dues, J. M. Adams, and G. A. Shinkle, “Combustion knock sensing: Sensor selection and application issues,” *SAE International*, 1990.
- [6] D. Scholl, T. Barash, S. Russ, and W. Stockhausen, “Spectrogram analysis of accelerometer-based spark knock detection waveforms,” *SAE International*, pp. 1183–1190, 1997.
- [7] L. Eriksson, *Spark advance modeling and control*. PhD thesis, Linköping University, 1999.
- [8] J. Frey and J. Peyton Jones, “Closed loop knock intensity characteristics of a classical knock control system,” *IFAC-PapersOnLine*, 2015.
- [9] J. Peyton Jones, K. R. Muske, and J. Frey, “A stochastic knock control algorithm,” *SAE International*, 2009.
- [10] J. Peyton Jones, J. M. Spelina, and J. Frey, “Likelihood-based control of engine knock,” *IEEE*, pp. 2169–2180, 2013.
- [11] A. Thomasson, L. Eriksson, T. Lindell, J. Peyton Jones, J. Spelina, and J. Frey, “Tuning and experimental evaluation of a likelihood-based engine knock controller,” 2013.
- [12] J. Peyton Jones, J. M. Spelina, and J. Frey, “Optimizing knock thresholds for improved knock control,” *International Journal of Engine Research*, pp. 123–132, 2014.
- [13] J. Peyton Jones, J. M. Spelina, and J. Frey, “Characterization of knock intensity distributions: Part 1: statistical independence and scalar measures,” *Journal of Automobile Engineering*, pp. 117–128, 2013.
- [14] S. Shayestehmanesh, J. Peyton Jones, and J. Frey, “Stochastic characteristics of knock and imep,” *SAE International*, 2018.
- [15] J. Ghandi and K. Kim, “A statistical description of knock intensity and its prediction,” *SAE International*, 2017.
- [16] W. Leppard, “Individual-cylinder knock occurrence and intensity in multicylinder engines,” *SAE International*, 1982.

- [17] J. Peyton Jones, J. M. Spelina, and J. Frey, "Control-oriented knock simulation," *SAE International*, 2016.
- [18] Abhijit and J. D. Naber, "Ionization signal response during combustion knock and comparison to cylinder pressure for si engines," *SAE International*, 2008.
- [19] K. Sinnerstad, "Knock intensity and torque control on svc engine," Master's thesis, Linköping University, 2003.
- [20] J. D. Naber and Jason R. Blough, "Analysis of combustion knock metrics in spark-ignition engines," *SAE International*, 2006.
- [21] G. Wu, "A real time statistical method for engine knock detection," *SAE International*, 2007.
- [22] J. M. Spelina, J. Peyton Jones, and J. Frey, "Characterization of knock intensity distributions: Part 2: parametric models," *Journal of Automobile Engineering*, pp. 1650–1660, 2013.
- [23] J. Frank and J. Massey, "The kolmogorov-smirnov test for goodness of fit," *Journal of the American Statistical Association*, 1951.
- [24] Y. Lonari, C. Polonowski, J. Naber, and B. Chen, "Stochastic knock detection model for spark ignited engines," *SAE International*, 2011.

# Appendix A

## Additional knock control results

---

Additional results from the knock control algorithms are shown in Section A.1, A.2, A.3 and A.4.

### A.1 Cumulative summation based knock control with likelihood-scaled control gains

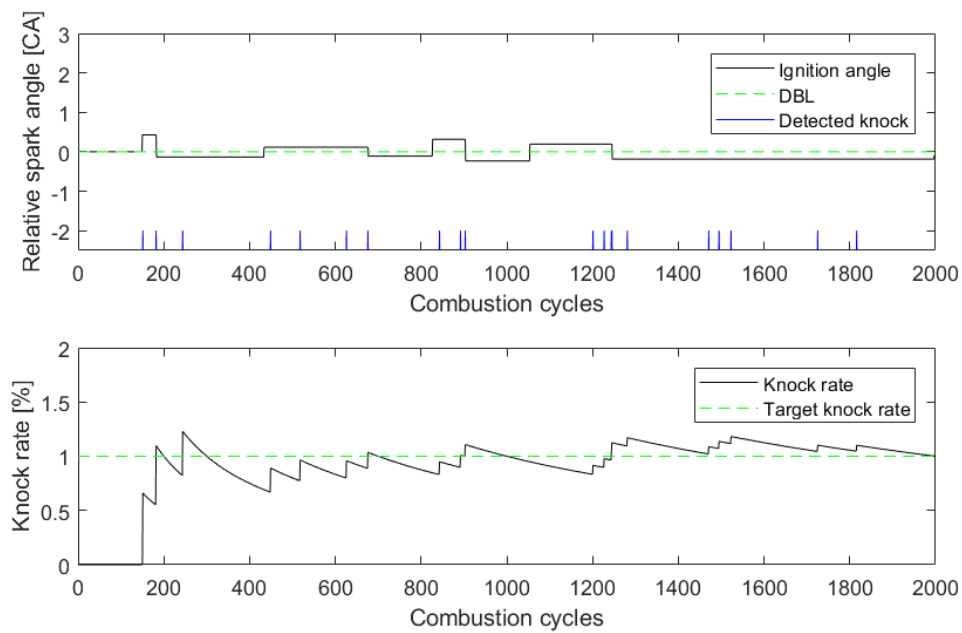


**Figure A.1:** Steady-state operation of the cumulative summation based knock controller with likelihood-scaled knock controller in the simulation environment.

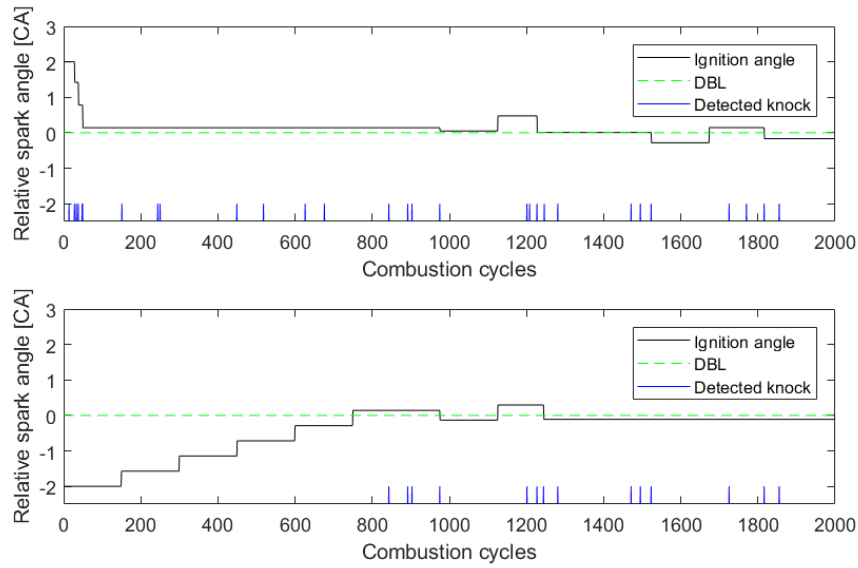


**Figure A.2:** Transient response of the cumulative summation based knock controller with likelihood-scaled knock controller in the simulation environment.

## A.2 Cumulative summation based knock control with fast forward algorithm and likelihood-scaled controller gains

The fast-forward algorithm to the cumulative summation controller decreased the distance to the lower boundary if consecutive ignition advancements was made.

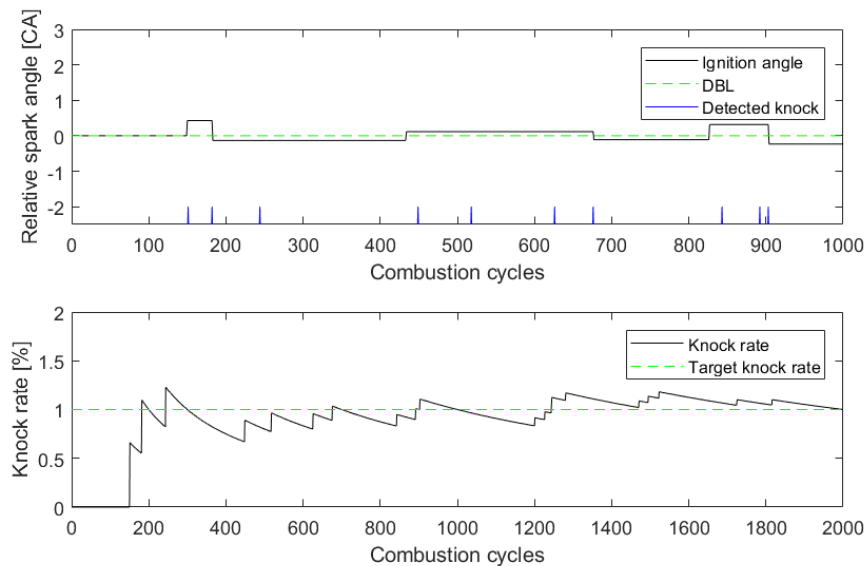


**Figure A.3:** Steady-state operation of the cumulative summation knock controller with fast forward algorithm and likelihood-scaled controller gains in the simulation environment. The ignition angle was initially set at  $\pm 2^\circ$  from DBL-timing.

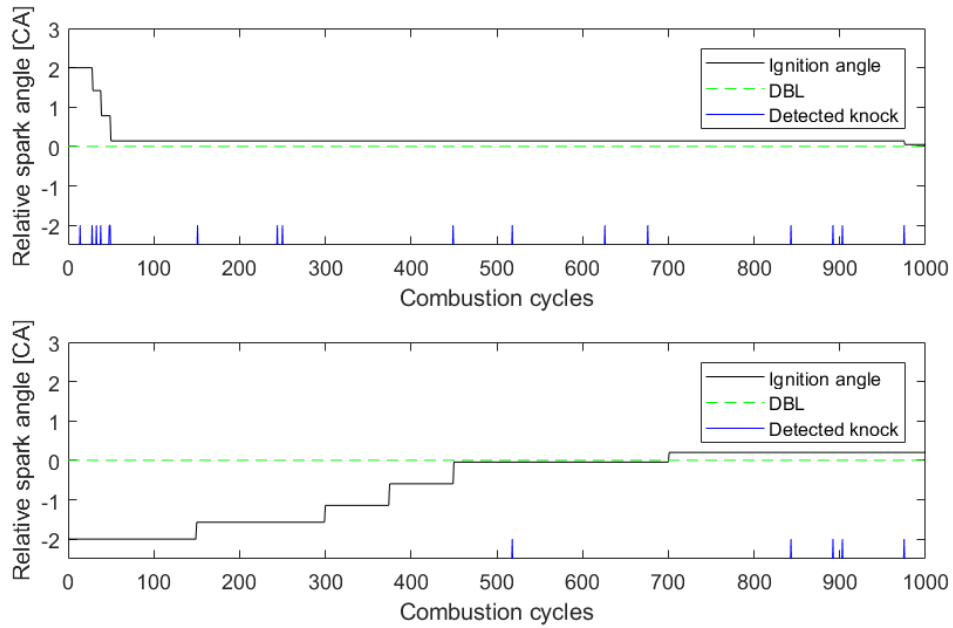


**Figure A.4:** Transient response of the cumulative summation knock controller with fast forward algorithm and likelihood-scaled controller gains in the simulation environment. Ignition angle with an initial spark angle disturbance of  $\pm 2^\circ$  CA from DBL-timing are shown.

### A.3 Likelihood knock control

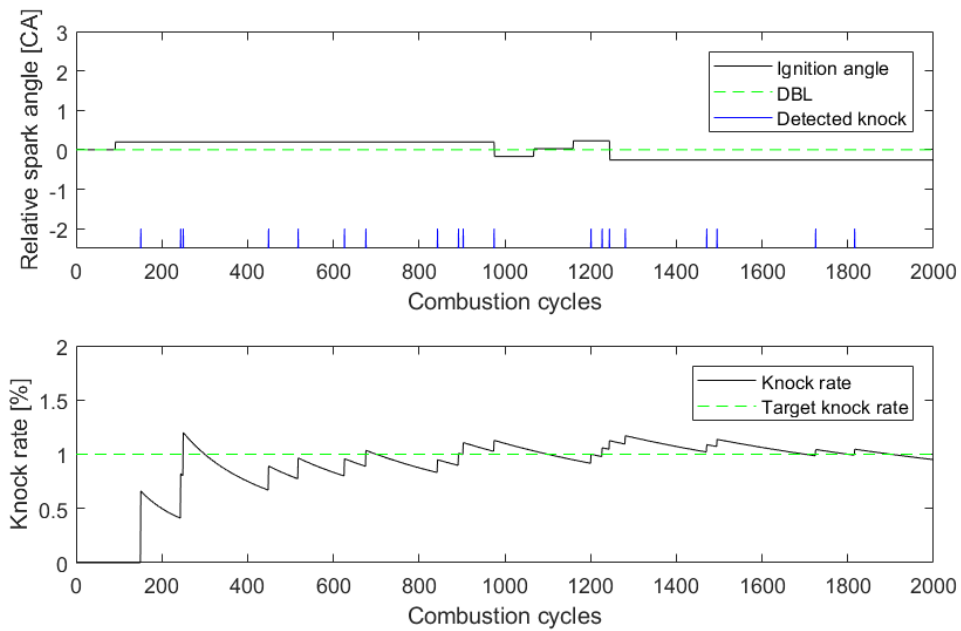


**Figure A.5:** Steady-state operation of the likelihood knock controller in the simulation environment.

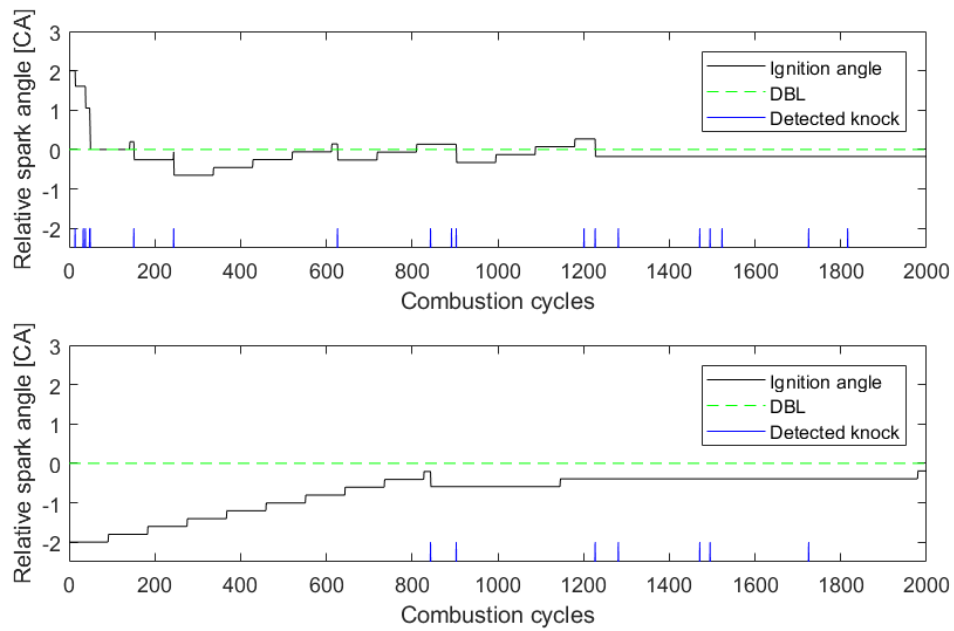


**Figure A.6:** Transient response of the Likelihood knock controller in the simulation environment with an initial spark angle disturbance of  $\pm 2^\circ$  CA from DBL-timing.

#### A.4 Live estimation controller

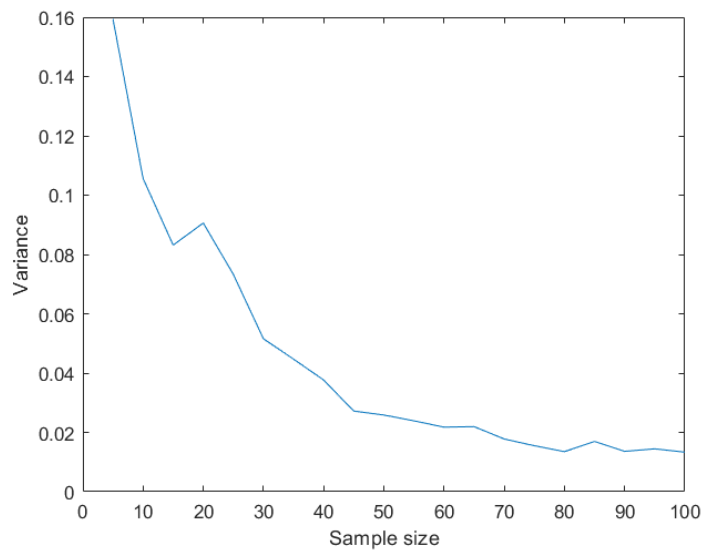


**Figure A.7:** Knock factor variance for different sample sizes in the knock intensity buffer. 200 distributions were estimated in each sample size.

# Appendix B

## Knock control results from real engine tests

---

Test results from real engine tests will be shown here. The operating condition for all tests were 2000rpm, 500mgair/stroke and an air-fuel ratio such that  $\lambda = 1$  was aimed to be achieved.

### B.1 Cumulative summation knock control with likelihood-scaled controller gains and optimised threshold

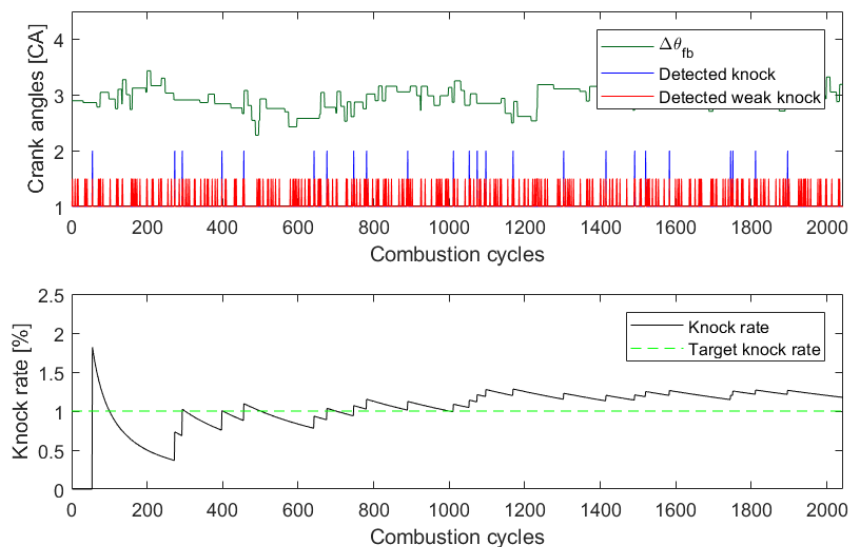


**Figure B.1:** Steady-state operating test for the threshold optimised cumulative summation knock controller with likelihood-scaled gains in a real engine.

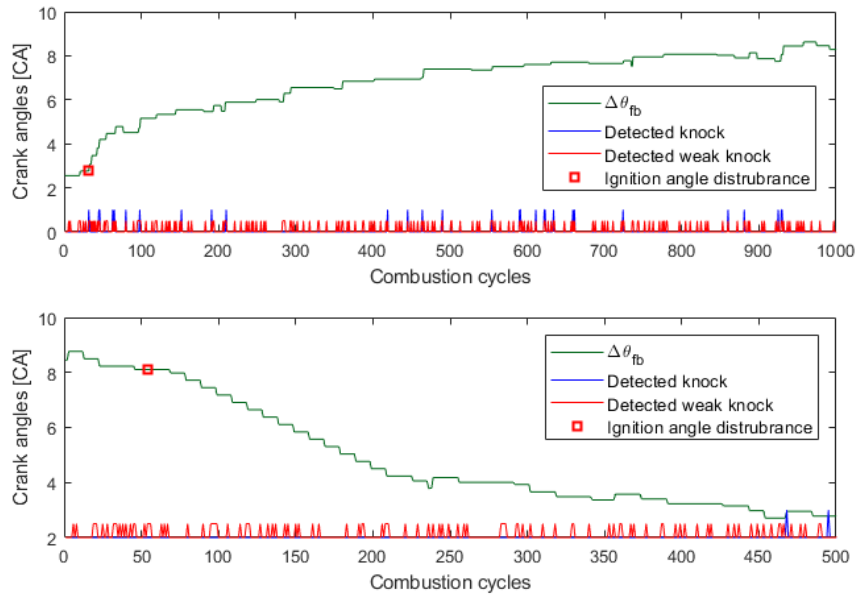


**Figure B.2:** Transient response for the threshold optimised cumulative summation controller with likelihood-scaled controller gains in real engine test. The controller was given a challenging task with offset of  $\pm 6$  degrees. The top most plot shows how the controller retards the feedback ignition angle and the bottom most shows how the controller advances the feedback signal.

## B.2 Threshold optimised conventional controller

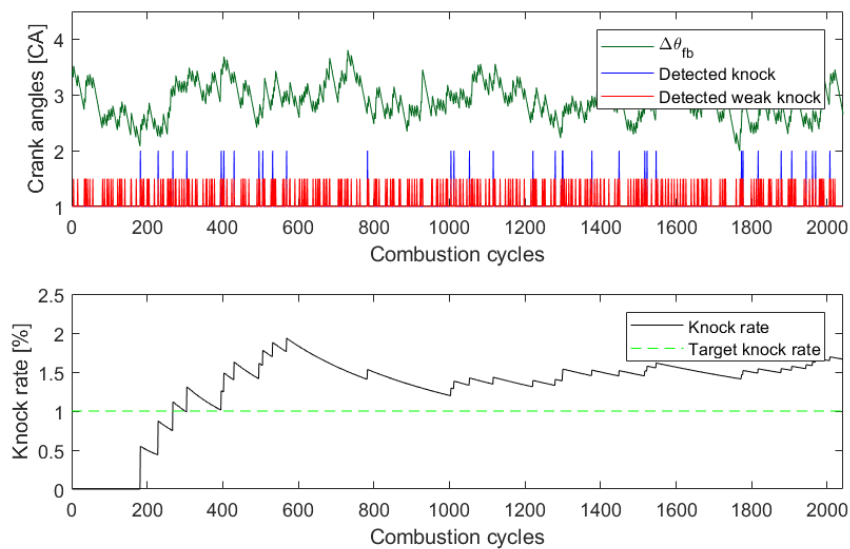


**Figure B.3:** Steady-state real engine test for the conventional controller with optimised threshold. Ignition feedback from the knock controller and knock rate are shown for a test were about 2000 combustion cycles were executed.

### B.3 Likelihood fast forward controller

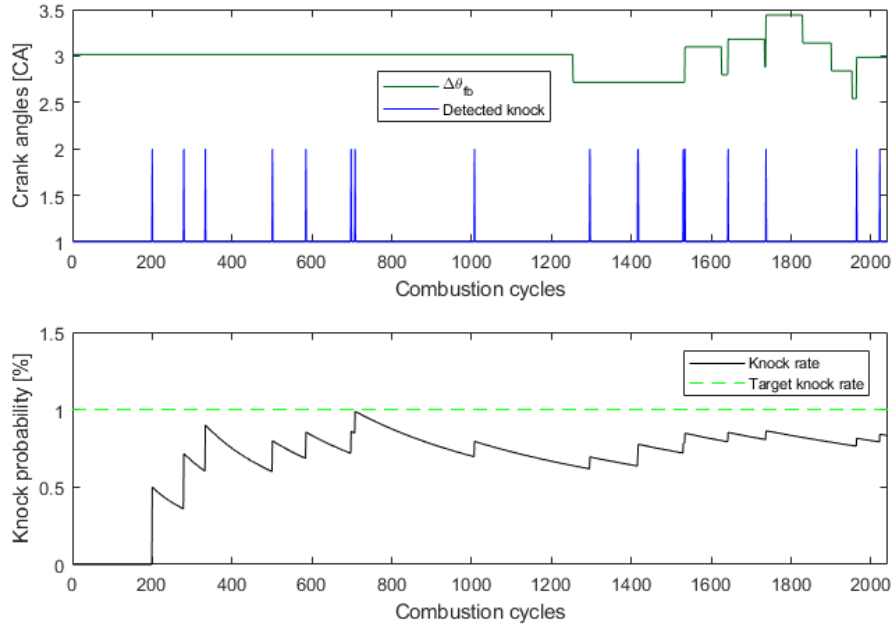


**Figure B.4:** Steady-state Results from a test of a real engine implemented with the likelihood controller with fast forward algorithm.

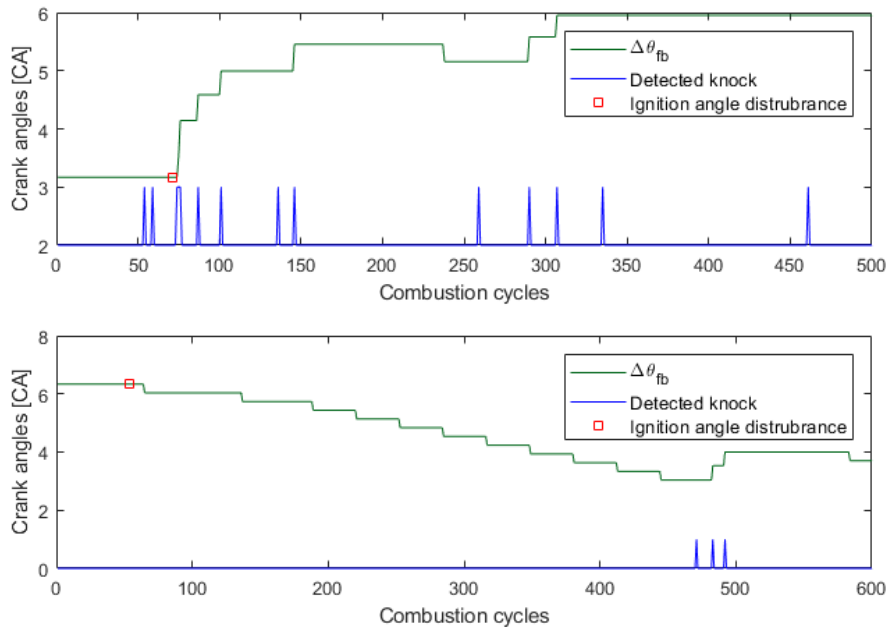


**Figure B.5:** Transient response of the Likelihood controller with fast forward add on from real engine test. Ignition angle offsets of  $\pm 3^\circ$  CA were performed.